

## **ABSTRACT**

Title of Document: CHARACTERIZATION OF FR-4 PRINTED  
CIRCUIT BOARD LAMINATES BEFORE  
AND AFTER EXPOSURE TO LEAD-FREE  
SOLDERING CONDITIONS

Ravikumar Sanapala, Master of Science, 2008

Directed By: Chair Professor, Michael G. Pecht, Department  
of Mechanical Engineering

The transition to lead-free soldering of printed circuit boards (PCBs) using solder alloys such as Sn/Ag/Cu has resulted in higher temperature exposures during assembly compared with traditional eutectic Sn/Pb solders. The knowledge of possible variations in the PCB laminate material properties due to the soldering conditions is an essential input in the selection of appropriate laminates.

An experimental study was conducted to investigate the effects of lead-free processing on key thermomechanical, physical, and chemical properties of a range of FR-4 PCB laminate materials. The laminate material properties were measured as per the IPC/UL test methods before and after subjecting to multiple lead-free soldering cycles.

The effect of lead-free soldering conditions was observed in some of the material types and the variations in properties were related to the material constituents. Fourier transform infrared (FTIR) spectroscopy and combinatorial property analysis were performed to investigate the material-level transformations due to soldering exposures.

CHARACTERIZATION OF FR-4 PRINTED CIRCUIT BOARD LAMINATES  
BEFORE AND AFTER EXPOSURE TO LEAD-FREE SOLDERING  
CONDITIONS

By

Ravikumar Sanapala

Thesis submitted to the Faculty of the Graduate School of the  
University of Maryland, College Park, in partial fulfillment  
of the requirements for the degree of  
Master of Science,  
Mechanical Engineering.  
August, 2008

Advisory Committee:

Dr. Michael Pecht, Chair Professor of Mechanical Engineering  
Dr. Patrick McCluskey, Associate Professor, Mechanical Engineering  
Dr. Peter Sandborn, Associate Professor, Mechanical Engineering  
Dr. Diganta Das, Faculty Research Scientist, Mechanical Engineering

© Copyright by  
Ravikumar Sanapala  
2008

## **Dedication**

I wish to dedicate this thesis to my parents for their unconditional love and support  
through out my life

## **Acknowledgements**

I would like to express my sincere gratitude to my advisor, Prof. Michael Pecht, for giving me the opportunity to be involved in this experimental study, and for all his support and guidance. I am also very much indebted to Bhanu Sood for his consistent supervision and productive discussion on my work. I also thank Dr. Diganta Das for his helpful insights on giving directions to my thesis and constant guidance throughout my stay at University of Maryland. I wish to extend my thanks to Dr. Patrick McCluskey and Dr. Peter Sandborn for serving on my thesis committee and reviewing my work.

I want to personally thank Dr Michael Azarian for his valuable inputs related to my thesis. I would like to thank all the CALCE EPS consortium members for their support in performance of this study. I also appreciate and acknowledge the inputs from Louis Lin of NanYa Plastics Corporation, Taiwan, and Joe Beers of Gold Circuit Electronics, USA, during the course of my thesis.

Lastly, I wish to express my thanks to all my friends and faculty at CALCE for making it an enjoyable place to work.

# Table of Contents

Dedication.....	ii
Acknowledgements.....	iii
Table of Contents.....	iv
List of Tables.....	vi
List of Figures.....	vii
Chapter 1: Introduction.....	1
1.1 Overview of PCB fabrication.....	1
1.2 Literature Review.....	3
1.3 Objectives of Thesis.....	6
1.4 Overview of Thesis.....	6
Chapter 2: Constituents of FR-4 Laminates.....	8
2.1 Reinforcement.....	8
2.2 Resin system.....	9
2.2.1 Curing agents.....	10
2.2.2 Flame retardants.....	12
2.2.3 Fillers.....	13
2.2.4 Accelerators.....	13
Chapter 3: Test Materials and Exposure Conditions.....	14
3.1 Test materials.....	14
3.2 Material construction.....	17
3.3 Exposure conditions.....	18
Chapter 4: Material Properties and Test Methods.....	20
4.1 Glass transition temperature ( $T_g$ ).....	20
4.2 Coefficient of thermal expansion (CTE).....	22
4.3 Decomposition temperature ( $T_d$ ).....	25
4.4 Time-to-delamination (T-260).....	26
4.5 Water absorption.....	28
4.6 Flammability.....	28
Chapter 5: Results and Discussion.....	31
5.1 Glass transition temperature ( $T_g$ ).....	31
5.2 Coefficient of thermal expansion (CTE).....	33
5.3 Decomposition temperature ( $T_d$ ).....	36
5.4 Time-to-delamination (T-260).....	40
5.5 Water absorption.....	41
5.6 Flammability.....	42
Chapter 6: Analysis of Results.....	45
6.1 Fourier transform infrared (FTIR) spectroscopy analysis.....	45
6.1.1 Introduction.....	45
6.1.2 Analysis.....	47
6.2 Combinatorial property analysis.....	52
Chapter 7: Summary and Conclusions.....	55
Chapter 8: Contributions.....	57

Appendix I: Datasheet values for the material properties studied .....	58
Appendix II: FTIR spectra of control and 6X reflowed samples of material B .....	59
Bibliography .....	60

## List of Tables

Table 1: Some of the common PCB material types [4] .....	2
Table 2: Typical constituents of FR-4 laminates .....	8
Table 3: Typical constituents of E-Glass [4] .....	9
Table 4: Laminate material classification .....	15
Table 5: EDS analysis of laminates .....	16
Table 6: Material properties and test methods .....	20
Table 7: The $T_g$ comparison between DSC and TMA methods .....	33
Table 8: Control in-plane (warp and fill) CTE measurement results.....	35
Table 9: Post exposure in-plane (warp) CTE measurement results.....	35
Table 10: Post exposure in-plane (fill) CTE measurement results .....	36
Table 11: Typical functional groups and wave numbers present in epoxy systems...	48
Table 12: Summary of variations in properties for materials B and H.....	52

## List of Figures

Figure 1: Typical steps involved in FR-4 printed circuit assembly fabrication.....	2
Figure 2: Typical glass-weave styles used in PCBs.....	9
Figure 3: Formation of DGEBA [4].....	10
Figure 4: Tetra-functional and multi-functional epoxy monomers [4].....	10
Figure 5: Typical structures of DICY and phenolic-cured resin systems [15] .....	11
Figure 6: Chemical structure of Tetrabromobisphenol A (TBBPA) .....	12
Figure 7: Chemical structure of DOPO (9, 10-Dihydro-9-oxa-10-phosphophenanthren-10-oxide) .....	13
Figure 8: Chemical structure of Imidazole .....	13
Figure 9: ESEM picture showing filler particles in material B .....	16
Figure 10: Flow of test materials .....	17
Figure 11: 6-ply laminate structure.....	18
Figure 12: 12 layered fabricated board structure .....	18
Figure 13: Lead-free reflow profile used for the exposures .....	19
Figure 14: Perkin Elmer DSC .....	21
Figure 15: Glass transition temperature measurement plot (material J).....	22
Figure 16: Perkin Elmer TMA .....	23
Figure 17: Out-of-plane CTE measurement plot (material B).....	23
Figure 18: In-plane CTE (warp) measurement plot (material B) .....	24
Figure 19: In-plane CTE (fill) measurement plot (material B).....	24
Figure 20: Shimadzu TGA 50.....	25
Figure 21: Decomposition temperature measurement plot (material F).....	26
Figure 22: T-260 measurement plot (material B) .....	27
Figure 23: Typical PCB combustion steps [31].....	29
Figure 24: Test set up for flammability measurement .....	30
Figure 25: Effect of lead-free soldering exposures on $T_g$ of the laminates.....	32
Figure 26: Effect of lead-free soldering exposures on out-of-plane CTE of the laminates .....	34
Figure 27: Effect of lead-free soldering exposures on $T_d$ of the laminates .....	36
Figure 28: $T_d$ comparison between materials A and J .....	37
Figure 29: $T_d$ comparison between materials A and G1 .....	37
Figure 30: Effect of type of curing agent on $T_d$ of the laminates .....	38
Figure 31: $T_d$ comparison between materials C1 and C2 .....	38
Figure 32: Effect of presence of fillers on $T_d$ of the laminates.....	39
Figure 33: $T_d$ comparison between materials A and B .....	39
Figure 34: $T_d$ comparison between materials H and I.....	40
Figure 35: Effect of type of flame retardant on $T_d$ of the laminates .....	40
Figure 36: Effect of lead-free soldering exposures on T-260 of the laminates .....	41
Figure 37: Effect of lead-free soldering exposures on water absorption.....	42
Figure 38: Effect of lead-free soldering exposures on flammability of the laminates (total burning time) .....	43
Figure 39: Effect of lead-free soldering exposures on flammability of the laminates (Average burning time).....	43
Figure 40: Common molecular bending movements [38] .....	46

Figure 41: Typical functional groups present in the epoxy laminate systems .....	50
Figure 42: FTIR spectrum of control sample with functional groups identified (material H).....	51
Figure 43: FTIR spectra of a control and 6X reflowed sample (material H).....	51
Figure 44: Effect of baking on the $T_g$ of laminates.....	54

## **Chapter 1: Introduction**

Printed circuit boards (PCBs) are the baseline in electronic packaging upon which electronic components are formed into electronic systems. The directive on Restriction of certain hazardous substances (RoHS) [1], and the Waste electrical and electronic equipment (WEEE) directive [2] have led to the adoption of lead-free soldering conditions in the PCB assembly process. The drive towards lead-free electronics has resulted in the use of lead-free solders in the PCB assembly. Common lead-free solder alloys such as Sn/Ag/Cu and Sn/Ag typically require a peak reflow temperature increase of 30-40°C for longer time periods compared to eutectic Sn/Pb reflow soldering conditions [3]. Rework and repair of assembled circuit boards also contribute to additional high temperature exposures. These exposures can alter the circuit board laminate material properties thereby creating a shift in the expected reliability of the PCB and the entire electronic assembly. The dependence of the laminate properties on the material constituents combined with the possible variations due to lead-free soldering exposures has not yet been extensively investigated.

### **1.1 Overview of PCB fabrication**

The basic building blocks of a PCB are composites of resin and reinforcement. A wide variety of resin and reinforcement types that are commonly used in the PCB industry are listed in Table 1. The nomenclature shown for each type of material corresponds to the grades developed by National Electrical Manufacturers Association (NEMA).

**Table 1: Some of the common PCB material types [4]**

Nomenclature	Reinforcement	Resin	Flame retardant
FR-2	Cotton paper	Phenolic	Yes
FR-3	Cotton paper	Epoxy	Yes
FR-4	Woven glass	Epoxy	Yes
CEM-1	Cotton paper/woven glass	Epoxy	Yes
CEM-2	Cotton paper/woven glass	Epoxy	No
CEM-3	Woven glass/matte glass	Epoxy	Yes

FR-4 PCB is a composite of epoxy resin with woven fiberglass reinforcement and it is the most widely used printed circuit board (PCB) material. The steps involved in the fabrication of FR-4 printed circuit assembly (PCA) are shown in Figure 1.

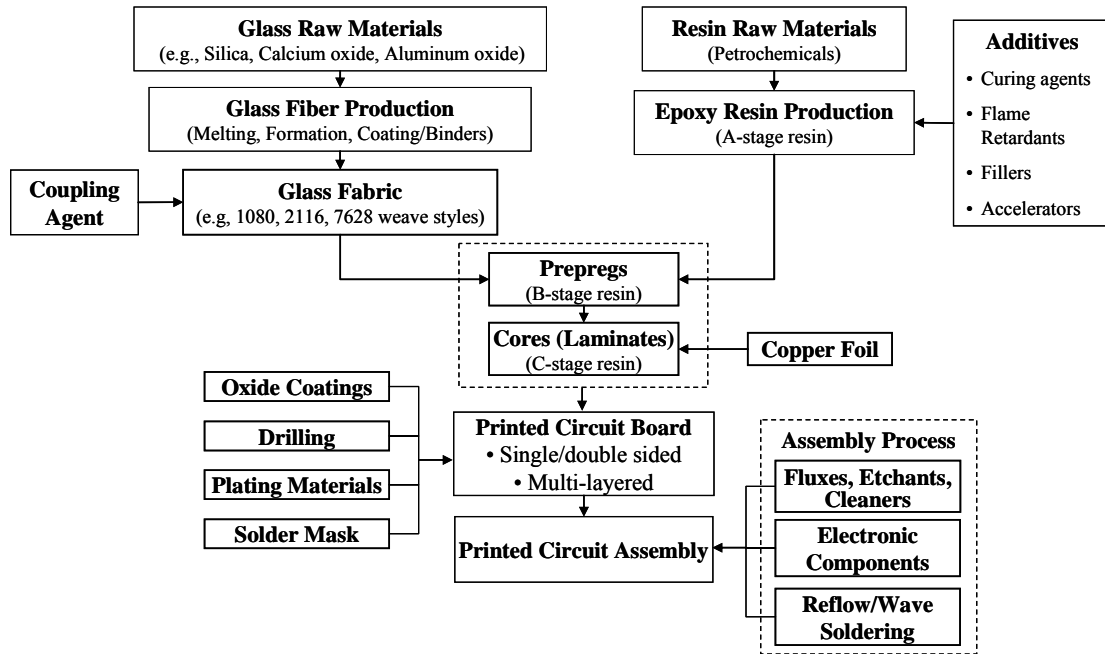


**Figure 1: Typical steps involved in FR-4 printed circuit assembly fabrication**

Glass raw materials are melted in a furnace and extruded to form fiberglass filaments that are combined into strands of multiple fiber yarn. Yarns are then weaved to form fiberglass cloth. A coupling agent, typically an organosilane, is coated onto the fabric to improve the adhesion between organic resin and inorganic glass. Resin is obtained from processing the petrochemicals and in its pure (uncured) form is called

A-stage resin. Additives such as curing agents, flame retardants, fillers, and accelerators are added to the resin to tailor the performance of the board.

A prepreg is fabricated from a glass fabric impregnated with the semi-cured (B-stage) epoxy resin. Multiple prepregs are thermally pressed to obtain a core or laminate (C-stage resin). Copper foil is then typically electrodeposited to obtain a copper clad laminate. Several prepregs and cores (with copper cladding etched as per the circuit requirements) are stacked together under temperature and pressure conditions to fabricate a multi-layered PCB. Through-holes and micro-via interconnects are drilled in the PCB as per the application specific design data and then plated with copper. Solder mask is applied on the board surface exposing the areas to be soldered. Flux is applied at regions where the electronic components are to be soldered. The boards are then subjected to reflow and/or wave soldering process depending upon the type of components (surface mount or through-hole) to obtain the printed circuit assembly.

## **1.2 Literature Review**

Very few studies were conducted to characterize FR-4 laminate materials and assess the variations in material properties due to multiple lead-free soldering profile exposures. Bergum [5] characterized some of the laminate materials (low  $T_g$  DICY & non-DICY-cured, mid  $T_g$  halogen-free, and high  $T_g$  DICY & non-DICY-cured) by analyzing the material properties such as glass transition temperature ( $T_g$ ), coefficient of thermal expansion (CTE), decomposition temperature ( $T_d$ ), and flexural modulus combined with their variations due to simulated thermal excursions. The thermal exposures were carried out by standard analytical techniques, such as differential

scanning calorimetry (DSC), thermomechanical analysis (TMA), dynamic mechanical analysis (DMA), and thermogravimetric analysis (TGA) to simulate the thermal excursions experienced by the laminates during assembly process. Multiple cycles were repeated on the same sample at peak temperatures of 235°C and 260°C to observe the variations in properties.

Kelley, *et al.*, ([6], [7]) reported the effect of thermal exposures associated with typical Sn/Pb and Sn/Ag/Cu reflow conditions on epoxy-based laminates by assessing the decomposition temperature. The laminates were exposed to multiple thermal cycles in TGA with peak temperatures of 235°C and 260°C and a change in the percentage weight loss of the sample was monitored. The study illustrated the possibility of rapid thermal degradation in the epoxy systems of conventional high  $T_g$  materials with repeated cycling at peak temperature of 260°C. The authors also demonstrated the usage of a methodology in the selection of lead-free compatible laminates for appropriate applications. The methodology was developed based on the PCB design features such as overall thickness, number of layers, copper foil weight, aspect ratio, resin content and process conditions such as number of reflow cycles. The study was focused on four types of laminate materials with different combinations of  $T_g$  and  $T_d$ .

Kelley [8] also illustrated the differences in four types of laminate materials (combination of low  $T_g$ , high  $T_g$ , low  $T_d$ , and high  $T_d$ ) by assessing the properties of  $T_g$ ,  $T_d$ , thermal expansion and time-to-delamination (T260/T288). The study also reported the evaluation of reliability of multilayered PCBs fabricated out of the four materials. Survivability of the boards with multiple lead-free soldering exposures was

assessed. Interconnect stress test (IST) was performed before and after exposure of the boards to multiple reflow cycles to estimate the effect of exposures on the reliability of PCBs.

Ehrler [9] in his study investigated the response of two types of DICY-cured epoxy laminate materials to lead-free reflow cycles by assessing the reliability with repeated reflow tests and thermal cycling tests. He demonstrated that the DICY-cured materials tested were not able to withstand the thermal stresses during lead-free soldering exposures

Christiansen *et al.*, [10] reported the comparative analysis on different types of epoxy-based laminate materials (high  $T_g$ , mid  $T_g$  and low  $T_g$ ; halogen-free and halogenated; DICY and non-DICY cured) by measuring the properties of  $T_g$ , CTE,  $T_d$ , and T260/T288.

Valette *et al.*, [11] have also followed the approach of characterizing epoxy laminates based on material properties such as  $T_g$ , CTE,  $T_d$ , dielectric constant and assessed the performance of certain laminates that have higher thermal stability and lower dielectric constant in comparison to conventional FR-4 laminates.

Pecht *et al.*, [12] characterized a range of PCB laminate materials (low  $T_g$  FR-4, high  $T_g$  FR-4, polyimide, cyanate ester, and bismaleimide triazine) based on the moisture absorption capability at various relative humidity and temperature levels.

Qi *et al.*, [13] assessed the effect of type of PCB material on the durability of solder joints by characterizing certain types of laminate materials (low  $T_g$  FR-4, high  $T_g$  FR-4, and polyimide).

### **1.3 Objectives of Thesis**

Based on the literature review, there have been few attempted studies that were conducted on characterizing certain types of FR-4 laminates and assessing the impact of lead-free soldering assembly conditions on reliability of printed circuit boards. To date, no comprehensive report is available on the effect of lead-free soldering exposures on laminate material properties. Furthermore, a wide variety of laminate types that are commercialized as ‘Lead-free process compatible’ are available recently and selection of appropriate laminates has been a challenge for the electronic industry. An insight into the laminate material constituents and variations in their material properties due to lead-free soldering exposures is essential in the selection of appropriate laminate materials. The broad objective of this thesis is to characterize a wide range of commercially available FR-4 PCB laminate materials and investigate the effects of lead-free processing on the thermomechanical, physical, and chemical properties. The analysis is aimed at correlating the properties to the material constituents of laminates.

### **1.4 Overview of Thesis**

The constituents of FR-4 laminates are discussed in Chapter 2. The test materials and construction is presented in Chapter 3. Lead-free soldering exposures namely, three reflow cycles, six reflow cycles, and combination of one wave and two reflow cycles, considered for this study are also discussed in Chapter 3. In Chapter 4, the definitions of the material properties and the measurement procedures as per IPC /UL test standards are discussed. Results and the discussion on the effect of lead-free

soldering exposures on the material properties are presented in Chapter 5. Chapter 6 consists of discussion on Fourier transform infrared spectroscopy (FTIR) analysis and combinatorial material property analysis to investigate the potential material-level transformations due to the soldering exposures. Summary and conclusions of the research are listed in Chapter 7. Research contributions are discussed in Chapter 8.

## Chapter 2: Constituents of FR-4 Laminates

The typical constituents of a FR-4 laminate are listed in Table 2 and are discussed in detail in the subsequent sections. Each of these constituents is important in its own, and in combination they determine the properties of the laminates.

**Table 2: Typical constituents of FR-4 laminates**

Constituent	Major function(s)	Example material(s)
Reinforcement	Provides mechanical strength and electrical properties	Woven glass (E-grade) fiber
Coupling agent	Bonds inorganic glass with organic resin and transfers stresses across the matrix	Organosilanes
Resin	Acts as a binder and load transferring agent	Epoxy (DGEBA)
Curing agent	Enhances linear/cross polymerization in the resin	Dicyandiamide (DICY), Phenol novolac (phenolic)
Flame retardant	Reduces flammability of the material	Halogenated (TBBPA) or Halogen-free (Phosphorous compounds)
Fillers	Reduces thermal expansion	Silica
Accelerators	Increases reaction rate, reduces curing temperature, controls cross-link density	Imidazole, Organophosphine

### 2.1 Reinforcement

The woven glass (generally E-grade) fiber cloth acts as reinforcement for the laminate, primarily providing mechanical strength and electrical properties. Glass fabric is woven with two sets of fiber yarns (fibers are combined into strands of multiple fiber yarn). Warp yarn fibers lie in the machine direction of the fabric while those of fill yarn lie perpendicular to the warp direction. The typical constituents of glass (E-grade) used in FR-4 laminates are shown in Table 3. The type of glass-weave style is defined by the parameters such as glass fiber bundle diameter, number of fiber bundles, and linear density of the fabric ([4], [14]). The difference in the fabric styles that are commonly used in PCBs (1080, 2116 and 7628 weave styles) is represented

in Figure 2. The order of decreasing fabric density and thickness of the fabric among the glass-weave styles shown is 7628>2116>1080.

**Table 3: Typical constituents of E-Glass [4]**

Constituent	Composition (%)
Silicon dioxide (SiO <sub>2</sub> )	52-56
Calcium oxide (CaO <sub>2</sub> )	16-25
Aluminum oxide (Al <sub>2</sub> O <sub>3</sub> )	12-16
Boron oxide (B <sub>2</sub> O <sub>3</sub> )	5-10
Sodium oxide (Na <sub>2</sub> O) + Potassium oxide (K <sub>2</sub> O)	0-2
Magnesium oxide (MgO)	0-5
Iron oxide (Fe <sub>2</sub> O <sub>3</sub> )	0.05-0.4
Titanium oxide (TiO <sub>2</sub> )	0-0.8
Fluorides	0-1

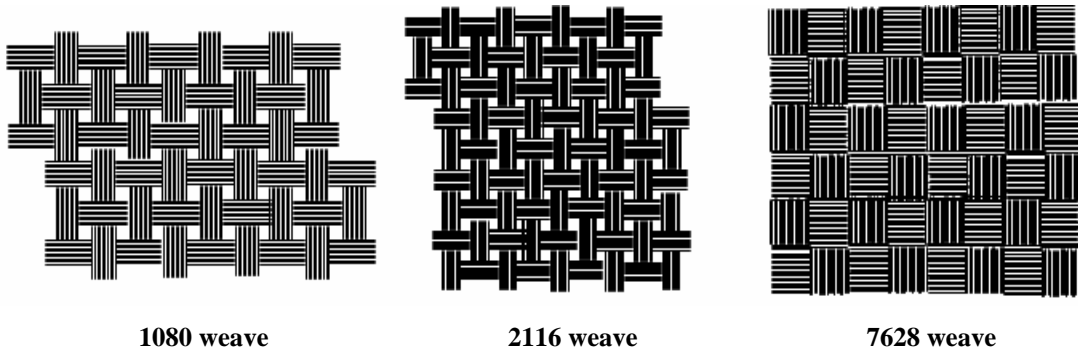


**Figure 2: Typical glass-weave styles used in PCBs**

## 2.2 Resin system

The resin system of a FR-4 laminate primarily consists of bi, tetra or multi-functional epoxy groups. Resin is derived from the reaction of Bisphenol-A with Epichlorohydrin which creates “Diglycidyl Ether of Bisphenol A” called DGEBA, also referred as Oxirane (shown in Figure 3). The epoxy groups present in DGEBA react in subsequent resin polymerization and result in curing of the resin system. Higher cross-linking in the cured system is achieved by the use of epoxy monomers with more than two epoxy functional groups per molecule (shown in Figure 4).

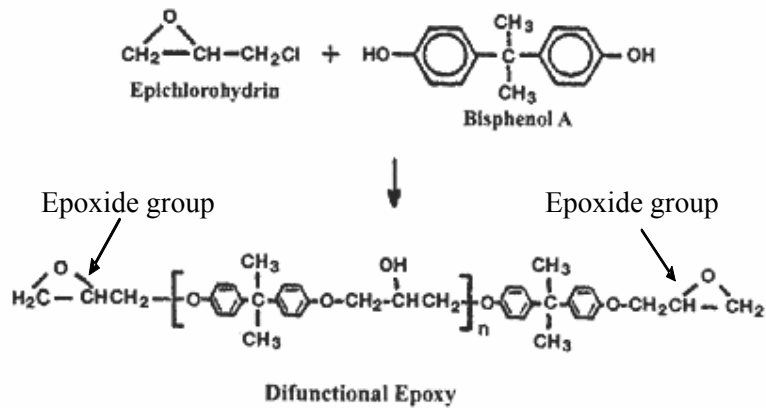


**Figure 3: Formation of DGEBA [4]**

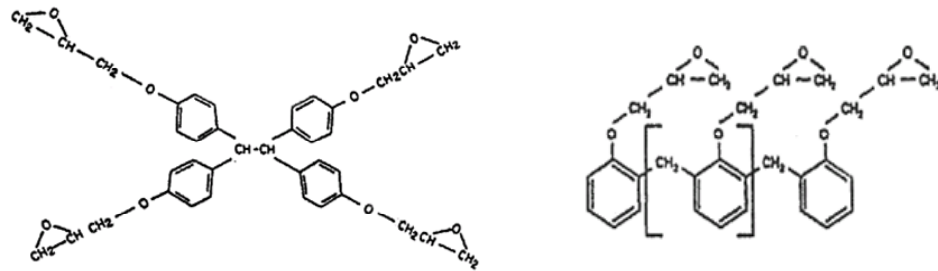


**Figure 4: Tetra-functional and multi-functional epoxy monomers [4]**

Additives such as curing agents, flame retardants, fillers, and accelerators are added to the resin system to improve the performance of laminate. These are added to the A-stage resin before prepreg fabrication.

### 2.2.1 Curing agents

Curing agents are added to the resin system to enhance cross-linking thereby thermosetting the composite structure. They are usually aliphatic or cycloaliphatic amines and polyamines or amides. Most widely used curing agents in the PCB industry are dicyandiamide (commonly known as DICY) and phenol novolac (phenolic). The chemical formulae of DICY and phenolic curing agents and typical molecular structures of the respective cured resin systems are shown in Figure 5.

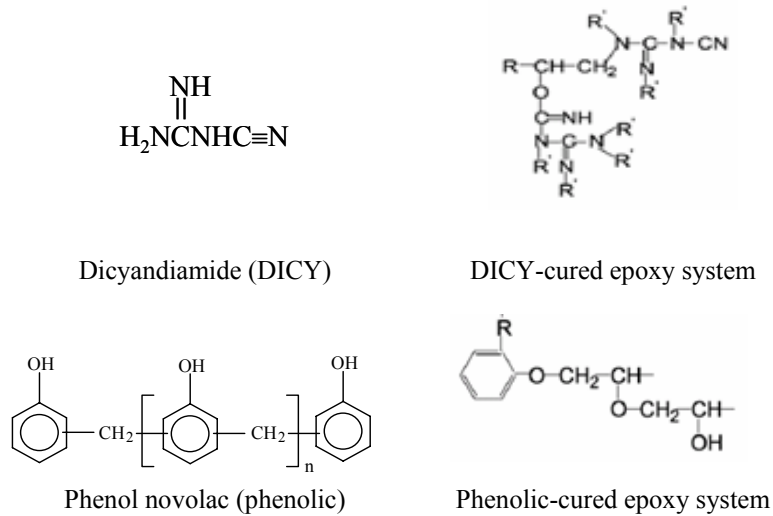


**Figure 5: Typical structures of DICY and phenolic-cured resin systems [15]**

The properties of DICY and phenolic cured systems differ because of the inherent differences in their molecular structures. DICY and its cured epoxy systems are linear aliphatic molecules compared to the aromatic structure of phenolic and its cured epoxy systems. This makes the phenolic-cured systems to be more thermally stable than DICY-cured systems. DICY-cured systems are more hydrophilic than phenolic-cured systems due to the presence of highly polar carbamidine-carbamide bond in their chemical structure. Also, at higher temperatures the strong polar nitrogen atom present in the DICY-cured system can destabilize the brominated epoxy resin resulting in the production of corrosive bromide ions. Overall, phenolic-cured resin systems offer better thermal resistance, chemical resistance, humidity resistance and improved mechanical properties but poor processability (e.g., drilling) compared to DICY-cured systems [15].

### 2.2.2 Flame retardants

Flame retardants are added to the resin system to reduce flammability of the laminate material. Tetrabromobisphenol-A (TBBPA) is the most commonly used halogenated (brominated) flame retardant for epoxy resin systems. The chemical structure of TBBPA is shown in Figure 6. Brominated flame retardants decompose during ignition, and retard combustion by trapping radicals generated from resins and by forming gas-phase barriers against oxygen [16].

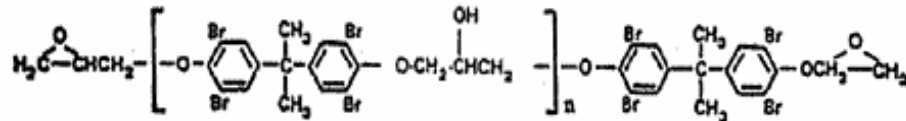


**Figure 6: Chemical structure of Tetrabromobisphenol A (TBBPA)**

Halogen-free flame retardant epoxy systems are gaining importance recently because of the shift in market trends to halogen-free products due to the public consciousness of the hazardous halogenated products, the industrial end user initiatives and the environmental legislations. Phosphorous compounds (such as Organophosphate esters) and metal hydroxides (such as Aluminum hydroxide and Magnesium hydroxide) are some of the commonly used halogen-free flame retardants. Organophosphate esters work by forming flame retarding glass-like barriers on the resin surface during ignition thereby cutting off oxygen necessary for combustion ([17], [18], [19]). The chemical structure of one of the most commonly used organophosphate ester (DOPO) is shown in Figure 7. Metal hydroxides retard flames by absorbing the heat during ignition, when added in large amounts [20].

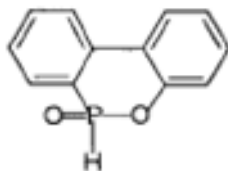


**Figure 7: Chemical structure of DOPO (9, 10-Dihydro-9-oxa-10-phosphophenanthren-10-oxide)**

### 2.2.3 Fillers

Fillers are added to the resin system for specific performance requirements such as lowering out-of-plane coefficient of thermal expansion (CTE) and to prevent barrel cracks in plated through holes. Fillers are also added to enhance the flame retardancy to meet UL 94V-0 flammability rating and to reduce material costs (as they replace resin). Typical fillers used in FR-4 PCBs are Silica and Aluminum silicate.

### 2.2.4 Accelerators

Accelerators are added to the resin system to increase the curing rate, reduce curing temperature and control cross-link density. Imidazole is one of the commonly used accelerators in FR-4 PCBs. The chemical structure of Imidazole is shown in Figure 8.

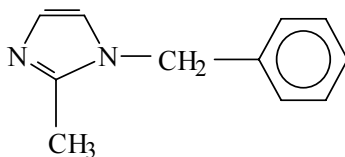


**Figure 8: Chemical structure of Imidazole**

## Chapter 3: Test Materials and Exposure Conditions

Laminate material classification, material construction and lead-free soldering exposure conditions used for the study are discussed in the following subsections.

### 3.1 Test materials

Fourteen commercially available FR-4 PCB laminates from two suppliers (I and II) were used in this study. The laminate materials used for the study were classified as shown in Table 4. Suppliers were chosen from different geographic locations with suppliers I and II from Taiwan and Japan respectively. Laminates were broadly categorized on the basis of their glass transition temperatures ( $T_g$ ) as high- $T_g$  ( $T_g > 165^\circ\text{C}$ ), mid- $T_g$  ( $140^\circ\text{C} < T_g < 165^\circ\text{C}$ ), and low- $T_g$  ( $T_g < 140^\circ\text{C}$ ) materials. Under each  $T_g$  category, laminates were grouped based on the type of curing agent (dicyandiamide [DICY] or phenol novolac [phenolic]), presence or absence of fillers, and type of flame retardants (halogenated or halogen-free). Laminates marketed for the high frequency applications (materials E and K) were also considered for the study. Coupling agents and accelerators were not controlled in the laminate materials.

Laminates amongst the pairs C1/C2, D1/D2 and G1/G2 differ only in the presence of fillers. The difference between C1/C2 and G1/G2 pairs is the ratio of high  $T_g$  resin. Material pair C1/C2 has higher percentage of tetrafunctional high  $T_g$  resin than that of G1/G2. The material type C2 also has a higher percentage of fillers than G2. The rest of the formulations are same amongst C1/C2 and G1/G2.

**Table 4: Laminate material classification**

Supplier	Material ID	Material classification			
		Glass transition temperature ( $T_g$ )	Curing agent	Fillers	Halogen-free
I	A	High $T_g$ ( $T_g > 165^\circ\text{C}$ )	DICY	No	No
I	B			Yes	Yes
I	C1		Phenolic	No	No
I	C2			Yes	No
II	D1			No	No
II	D2		Yes	No	
II	E		Yes	Yes	
I	F	Mid range $T_g$ ( $140^\circ\text{C} < T_g < 165^\circ\text{C}$ )	DICY	Yes	Yes
I	G1		Phenolic	No	No
I	G2			Yes	No
II	H			Yes	No
II	I		Yes	Yes	
I	J	Low $T_g$ ( $T_g < 140^\circ\text{C}$ )	DICY	No	No
I	K			Yes	No

Electro dispersive spectroscopy (EDS) analysis of the laminates (shown in Table 5) revealed that the flame retardant used in all the halogen-free materials is a phosphorous based compound; whereas halogenated materials have brominated compounds. Also, the EDS analysis showed that the choice of type of fillers and flame retardants in the laminates varies from supplier to supplier. Halogenated laminates C2, G2 from supplier I and D2, H from supplier II contain silicon based fillers (probably  $\text{SiO}_2$ ). Halogen-free laminates B, F from supplier I contain silicon and aluminum based fillers (probably  $\text{SiO}_2$ ,  $\text{Al}(\text{OH})_3$ ), whereas only laminate E from supplier II contain silicon and aluminum based fillers. Laminate I do not contain silicon based fillers. Environmental scanning electron microscopy (ESEM) analysis on the laminates with fillers (shown in Figure 9 for material B) revealed the microstructure of the filler particles.

**Table 5: EDS analysis of laminates**

Supplier	Material ID	Material classification			Inorganic elements detected			
		Curing agent	Fillers	Halogen-free	Br	P	Si	Al
I	A	DICY	No	No	✓	-	-	-
I	B	DICY	Yes	Yes	-	✓	✓	✓
I	C1	Phenolic	No	No	✓	-	-	-
I	C2	Phenolic	Yes	No	✓	-	✓	-
II	D1	Phenolic	No	No	✓	-	-	-
II	D2	Phenolic	Yes	No	✓	-	✓	-
II	E	Phenolic	Yes	Yes	-	✓	✓	✓
I	F	DICY	Yes	Yes	-	✓	✓	✓
I	G1	Phenolic	No	No	✓	-	-	-
I	G2	Phenolic	Yes	No	✓	-	✓	-
II	H	Phenolic	Yes	No	✓	-	✓	-
II	I	Phenolic	Yes	Yes	-	✓	-	✓
I	J	DICY	No	No	✓	-	-	-
I	K	DICY	Yes	No	✓	-	-	-

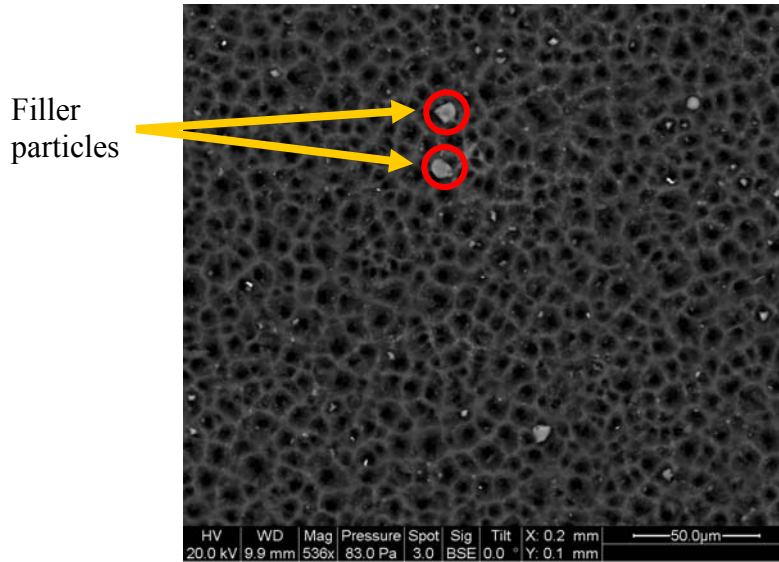


**Figure 9: ESEM picture showing filler particles in material B**

### 3.2 Material construction

The logistics involved in obtaining the materials for the study is shown in Figure 10. Laminates (cores) from supplier I and II with a nominal thickness of 1.2 mm and 1 oz (0.036 mm) copper cladding were considered for evaluating most of the properties.

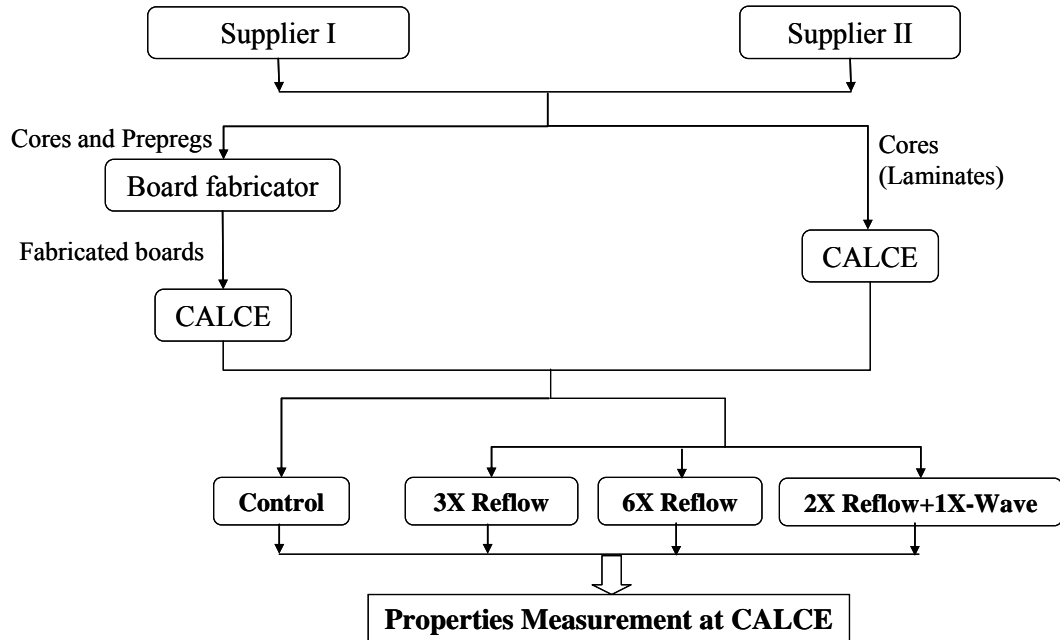


**Figure 10: Flow of test materials**

Laminates from supplier I have 6-ply of 7628 glass weave style with a resin content of 41%, and those from supplier II have 6-ply of 7629 glass weave style. Some of the property measurements require fabricated boards which were made at Gold circuit electronics, Taiwan. Fabricated boards consist of 12-layered stack up (nominal thickness of 2.5 mm, resin content: 53%) with alternative layers of cores and prepregs of 1080, 2116 and 7628 weave styles. Fabricated boards were available only for materials A, B, C1, C2, G1, J and they span the range of  $T_g$ , curing agents, flame retardants and fillers. The 6-ply structure of the cores and the 12-layered structure of the fabricated boards are represented in Figure 11.

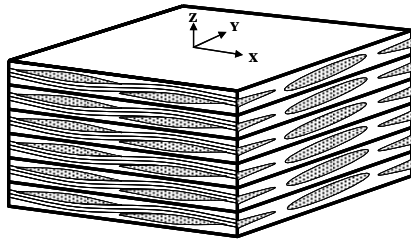


**Figure 11: 6-ply laminate structure**

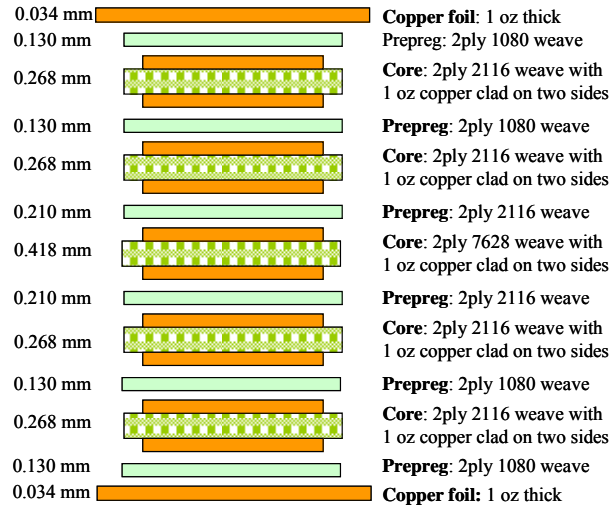


**Figure 12: 12 layered fabricated board structure**

The boards were designed as per the guidelines listed in IPC-4121 document [21]. The designed boards have a symmetric structure with 7628 weave style core at the center with 2116 and 1080 weave style cores and prepregs spreading outwards. The presence of finer weave fabrics with higher resin content on the outer surface and coarse weave fabrics with lower resin content on the inner layers also ensures better chemical resistance and resistance to measling (condition in which internal glass fibers are separated from the resin at the weave intersection) [21]. The inner layers consist of staggered circular copper etch pattern and the outer layers of copper do not have any etch pattern.

### 3.3 Exposure conditions

Laminate samples from all the material types were divided into four lots. The first lot refers to control and represents the samples as-received from the laminate suppliers. The second lot was exposed to three reflow cycles (3X-R), the third lot to six reflow cycles (6X-R), and the fourth lot to a combination of two reflow cycles and

one wave soldering cycle (2X-R+1X-W). The lead-free reflow test profile (measured using thermocouples placed at different locations on the first test board) is shown in Figure 13 and meets the IPC/JEDEC-J-STD-020D [22] recommended lead-free reflow profiles. For the lead-free wave soldering exposures, samples were passed through two preheat zones maintained at 175°C and 199°C respectively, followed by a lead-free solder (Sn96.5/Ag3.0/Cu0.5) wave at 295°C.

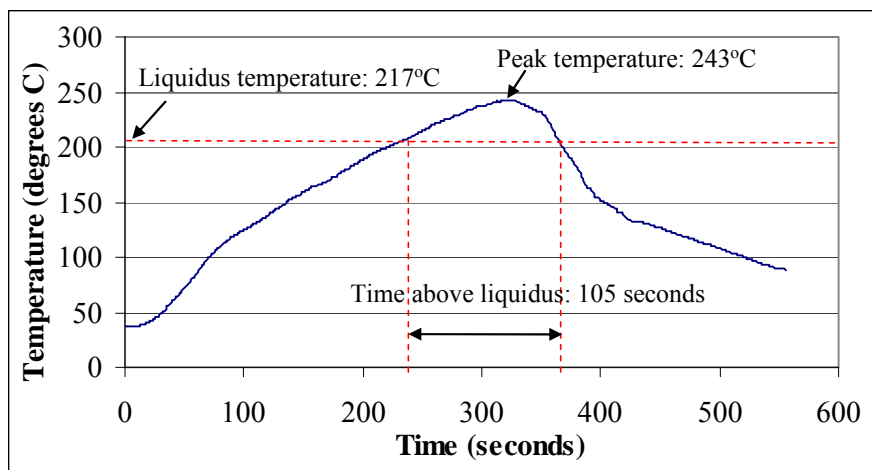


**Figure 13: Lead-free reflow profile used for the exposures**

## Chapter 4: Material Properties and Test Methods

The key thermomechanical, physical, and chemical properties of the PCB laminates considered for evaluation and the corresponding test methods are listed in Table 6. Previous studies ([5], [6], [8], [10]) have identified the properties of  $T_g$ , CTE,  $T_d$ , and T-260 as some of the primary metrics in assessing the lead-free process compatibility of laminates.

**Table 6: Material properties and test methods**

Property	Unit	Test method	Equipment
Glass transition temperature ( $T_g$ )	$^{\circ}\text{C}$	IPC-TM-650 2.4.25	Differential scanning calorimeter (DSC)
Coefficient of thermal expansion (CTE) (out-of-plane, in-plane)	ppm/ $^{\circ}\text{C}$	IPC-TM-650 2.4.24	Thermo mechanical analyzer (TMA)
Decomposition temperature ( $T_d$ )	$^{\circ}\text{C}$	IPC-TM-650 2.4.24.6	Thermo gravimetric analyzer (TGA)
Time-to-delamination (T-260)	min	IPC-TM-650 2.4.24.1	Thermo mechanical analyzer (TMA)
Water absorption	%	IPC-TM-650 2.6.2.1	Micro-balance
Flammability	sec	UL 94 (V-0)	Bunsen burner and gas supply

### 4.1 Glass transition temperature ( $T_g$ )

Glass transition temperature ( $T_g$ ) of a resin system is the temperature at which material transforms from rigid and glass like state to a rubbery and compliant state due to the reversible breakage of Van der Waals bonds between the polymer molecular chains. The  $T_g$  of a FR-4 laminate system primarily depends on the type of the epoxy resin and its percentage composition. Material properties such as

coefficient of thermal expansion, Young's modulus, heat capacity, and dielectric constant undergo a change around  $T_g$ .

The  $T_g$  of laminates was measured using Perkin-Elmer differential scanning calorimeter (Pyris 1 DSC) as per IPC-TM-650 2.4.25 test method [23]. The test equipment with the sample and reference containers is shown in Figure 14.

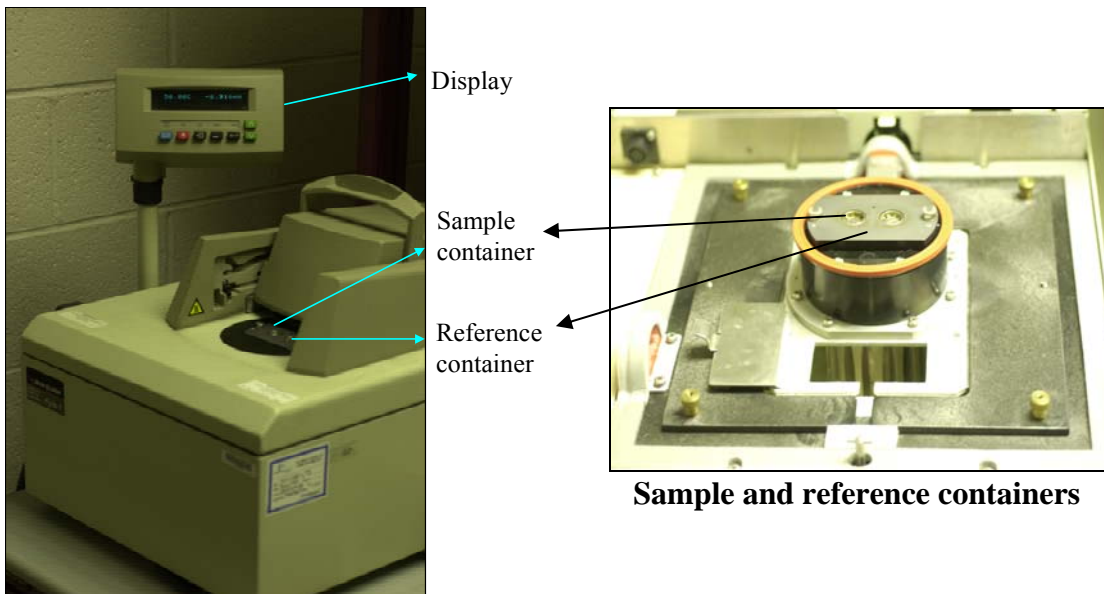


**Figure 14: Perkin Elmer DSC**

Two samples weighing between 15-30 mg were used for the measurements. Copper cladding was etched from the samples using sodium persulphate solution. Samples were then baked at 105°C for 2 hours and cooled to room temperature in a dessicator prior to the measurements. Samples were subjected to a temperature scan of 25°C to 220°C at a ramp rate of 20°C/min, and  $T_g$  was identified as the midpoint of step transition in the DSC measurement plot. The representative glass transition temperature measurement plot is shown in Figure 15.

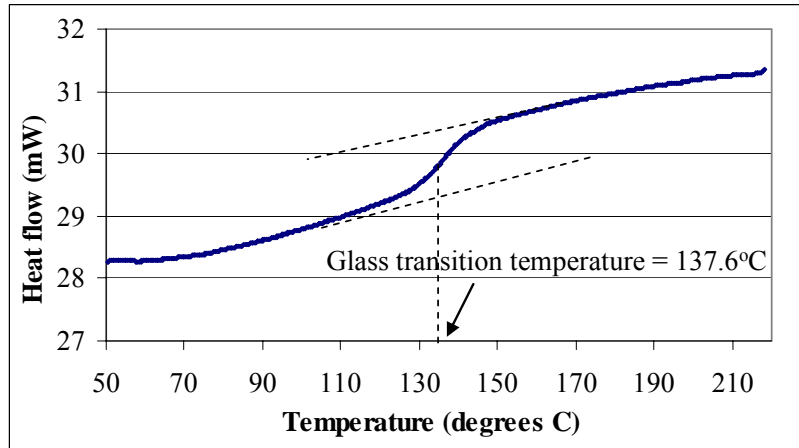


**Figure 15: Glass transition temperature measurement plot (material J)**

## **4.2 Coefficient of thermal expansion (CTE)**

Coefficient of thermal expansion (CTE) of a laminate is the fractional change of linear dimensions with temperature. Out-of-plane CTE influences failure mechanisms such as barrel cracking and delamination, whereas in-plane CTE in warp and fill directions affects shear failures of solder joints.

CTE of laminate materials in out-of-plane and in-plane directions were measured using Perkin-Elmer thermomechanical analyzer (Pyris TMA 7) as per IPC-TM-650 2.4.24 test method [24]. The test equipment used for the measurement is shown in Figure 16.

Two samples of 7 mm x 7 mm size were used for the measurements. Copper cladding was etched and the samples were baked at 105°C for 2 hours followed by cooling to room temperature in a desiccator prior to the measurements. Samples were subjected to a temperature scan of 25°C to 250°C at 10°C/minute ramp rate for out-of-plane CTE measurements, and 25°C to 220°C at 10°C/minute ramp rate for in-plane CTE measurements. The  $T_g$  was identified as the temperature at which slope of the

TMA measurement plot change, and CTE was measured below and above  $T_g$ . The representative out-of-plane and in-plane CTE (warp/fill) measurement plots are shown in Figure 17 to Figure 19.

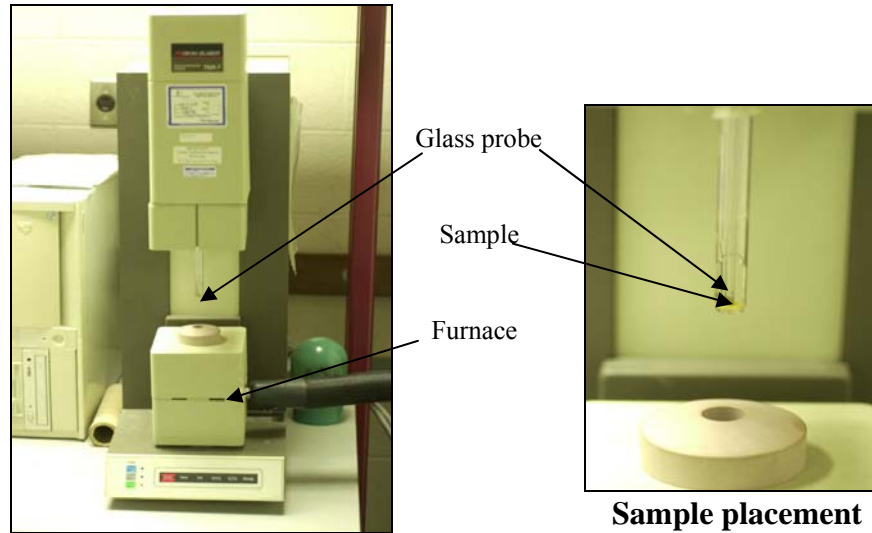


**Figure 16: Perkin Elmer TMA**

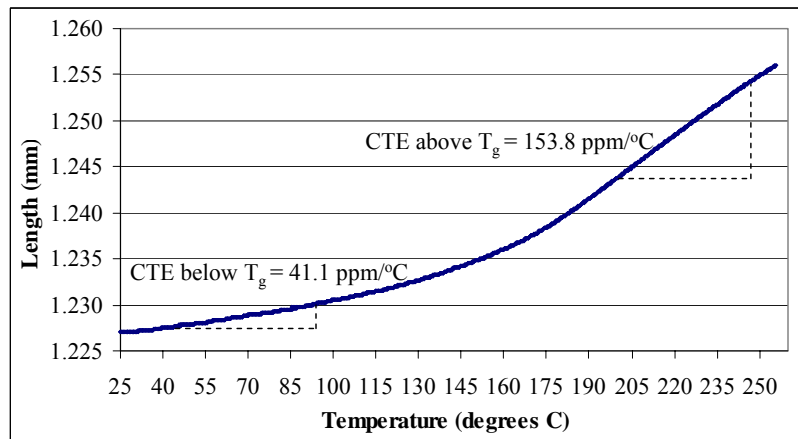


**Figure 17: Out-of-plane CTE measurement plot (material B)**

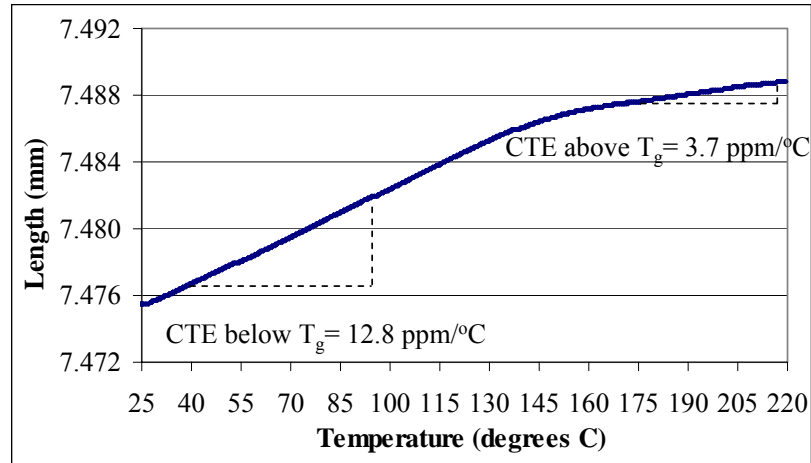


**Figure 18: In-plane CTE (warp) measurement plot (material B)**

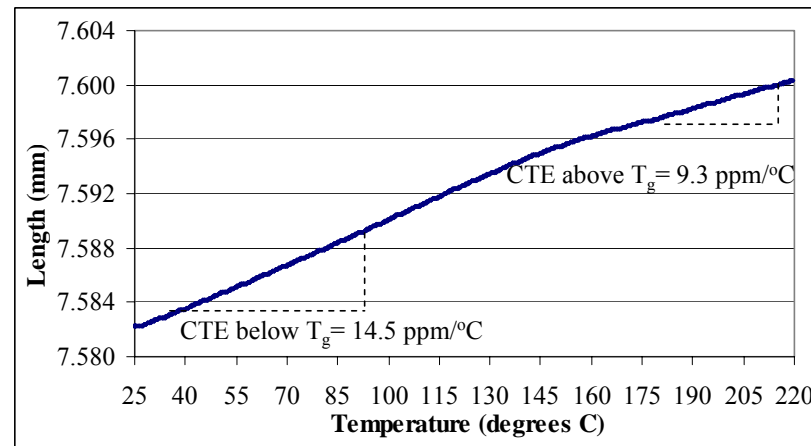


**Figure 19: In-plane CTE (fill) measurement plot (material B)**

The CTE of laminate materials in all the three directions (out-of-plane, warp and fill) is different. In-plane CTE (warp and fill) is less than out-of-Plane CTE as the former is dominated by the glass-fabric (typical CTE of E-glass: 5.4 ppm/°C [25]), whereas the latter is dominated by the epoxy resin (typical CTE of epoxy resin: 63 ppm/°C [25]). Also, epoxy resin behaving like an incompressible fluid is primarily constrained along the in-plane directions by the glass fabric [26].

In-plane CTE above  $T_g$  is lower compared to that of below  $T_g$  because of the significant reduction of Young's modulus of resin above  $T_g$  (below  $T_g$  Young's modulus of resin: 2.4 GPa, above  $T_g$  Young's modulus of resin: 0.07 GPa) [26]. Also,

epoxy acting as incompressible liquid when expanding along out-of-plane direction shrinks in the warp and fill directions. As the expansion rate along out-of-plane significantly increases above  $T_g$ , this may result in a reduction of above  $T_g$  in-plane CTE.

Difference between above  $T_g$  in-plane CTE and below  $T_g$  in-plane CTE along warp direction is higher than that along fill direction [27]. Changes in the tension and spacing of the warp and fill fiber bundles during weaving result in varying degrees of flexibility and hence different properties along the two directions [14].

### 4.3 Decomposition temperature ( $T_d$ )

Decomposition temperature ( $T_d$ ) is the temperature at which a resin system irreversibly undergoes physical and chemical degradation with thermal destruction of cross-links, resulting in weight loss of the material.

The  $T_d$  of laminates was measured using Shimadzu thermogravimetric analyzer (Shimadzu TGA 50) as per IPC-TM-650 2.4.24.6 test method [28]. The equipment used for the measurement is shown in Figure 20.

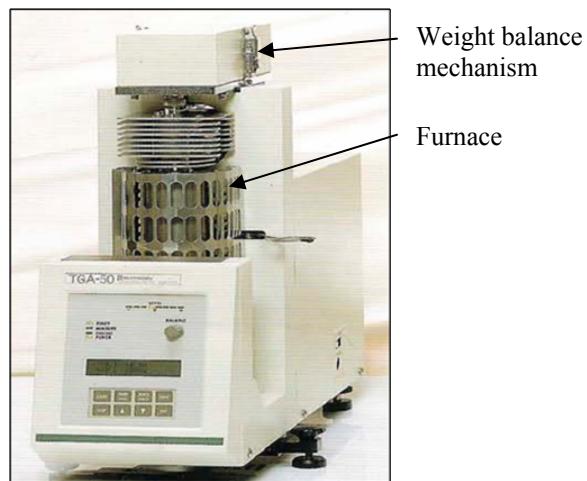


**Figure 20: Shimadzu TGA 50**

One test specimen from each material type weighing between 8-20 mg was used for the measurement. Copper cladding was etched and the samples were baked at 110°C for 24 hours followed by cooling to room temperature in a desiccator prior to the measurement. Sample was subjected to a temperature scan of 25°C to 400°C at a ramp rate of 10°C/minute in an inert nitrogen atmosphere (purged at 50 ml/minute). The change in weight of the sample was obtained as a function of temperature, and  $T_d$  was recorded at 2% and 5% weight loss (compared to sample weight at 50°C as per the test method). The representative decomposition temperature measurement plot is shown in Figure 21.

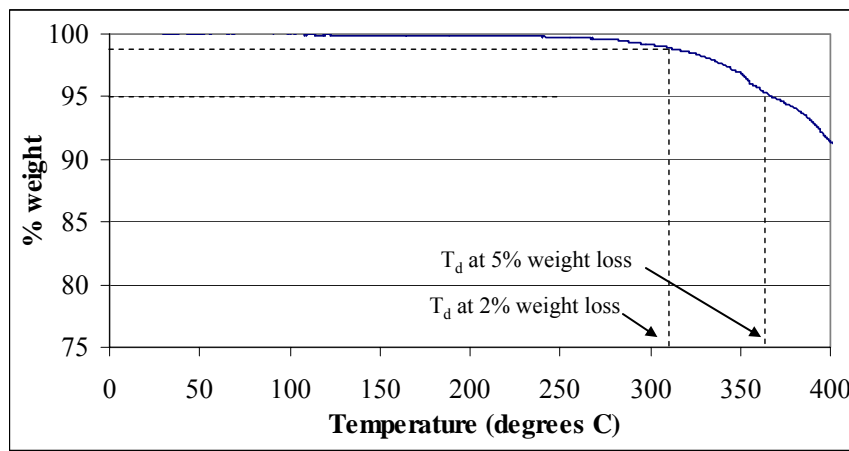


**Figure 21: Decomposition temperature measurement plot (material F)**

#### **4.4 Time-to-delamination (T-260)**

Time-to-delamination is the time taken by a laminate material to delaminate (separation between layers of prepregs and copper clad cores in a multilayered structure), when exposed to a constant temperature. Due to lead-free soldering process reaching peak temperatures of around 260°C, time-to-delamination measured at 260°C (T-260) is being used as a metric for assessing lead-free process

compatibility of laminates. It is a measure of the ability of a laminate material to withstand multiple soldering cycles without delamination.

The T-260 of fabricated boards was measured using Perkin-Elmer thermomechanical analyzer (Pyris TMA 7) as per IPC-TM-650 2.4.24.1 test method [29]. Two samples of 7 mm x 7 mm size were used for the measurements. Samples were baked at 105°C for 2 hours and then cooled to room temperature in a dessicator prior to the measurements. Samples were then subjected to a temperature scan of 25°C to 260°C at 10°C/minute ramp rate and held at 260°C until an irreversible change in thickness (assumed to be caused by layer to layer delamination) of the sample was observed. The test was terminated at 60 minutes for the laminate materials that did not delaminate until then. Time-to-delamination was determined as the time between onset of isotherm (260°C) and the onset of delamination. The representative T-260 measurement plot is shown in Figure 22.

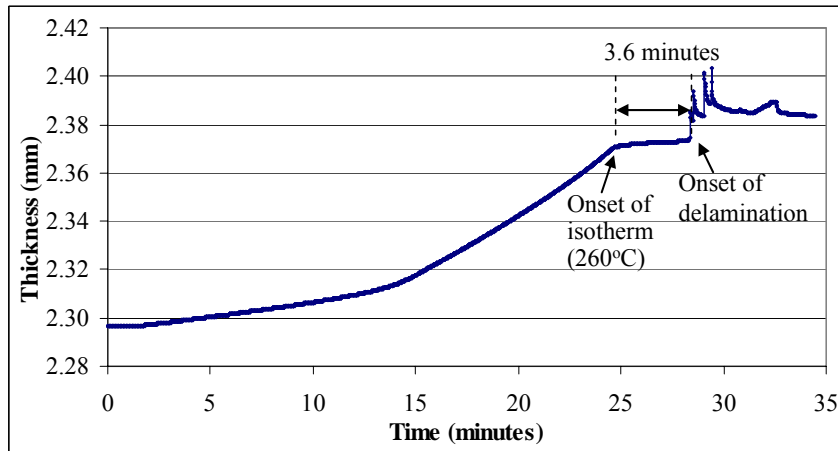


**Figure 22: T-260 measurement plot (material B)**

## 4.5 Water absorption

Water absorption is a measure of the amount of water absorbed by laminate materials when immersed in distilled water for 24 hours at room temperature. Water absorption of the laminates was measured as per IPC-TM-650 2.6.2.1 test method [30].

Three samples of 50 mm x 50 mm size were used for the measurements. Copper cladding was etched and the samples were baked at 105°C for 1 hour followed by cooling to room temperature in a dessicator prior to the measurements. Samples were weighed using microbalance before and after immersion in distilled water for 24 hours and percentage water absorption was calculated by the following expression:.

$$\% \text{ Water absorption} = \frac{\text{Wet weight} - \text{Conditioned weight}}{\text{Conditioned weight}} \times 100$$

## 4.6 Flammability

Flammability is a measure of the material's tendency to extinguish the flame once the specimen has been ignited and separated from the flame source. FR-4 PCB laminates, being plastics, are inherently flammable and flame retardants are added to the resin system in order to enhance their self-extinguishing property. Typical steps involved in a PCB combustion process are shown in Figure 23.

The flammability of laminates was measured as per UL 94 test method [32]. Five specimens per material type were cut into sizes of 127 mm x 12.7 mm. Copper cladding was etched and the samples were conditioned at 25°C, 50% relative humidity for 48 hours prior to testing.

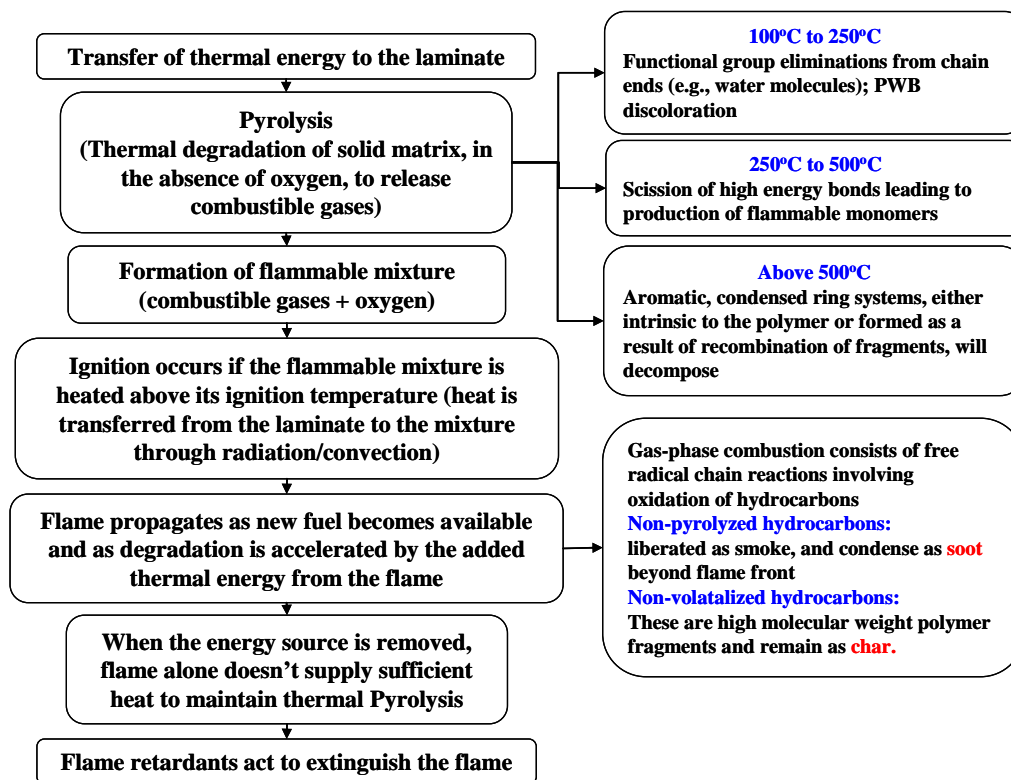
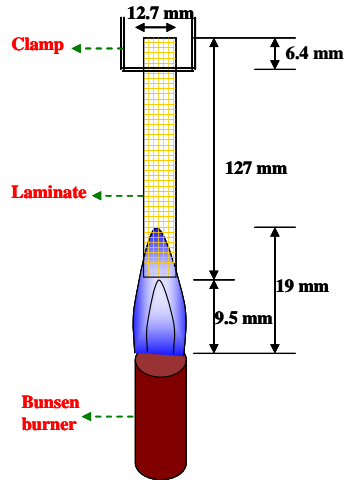


Figure 23: Typical PCB combustion steps [31]

Samples were ignited using a bunsen burner by a 19 mm high blue flame (as shown in Figure 24). Gas supply to the burner was adjusted to maintain the height. Flame was placed below the sample for 10 seconds and withdrawn. If active combustion ceases prior to specimen being completely consumed, samples were placed again for 10 seconds and withdrawn. Following parameters were noted: duration of the specimen burning after the first flame application, duration of the specimen burning after the second flame application, and if any specimen burns up the holding clamp on any ignition. Total specimen burning time was then calculated by summing the burning times in both flame applications.



**Figure 24: Test set up for flammability measurements**

The test results were compared against UL 94 V-0 flammability criteria, according to which, the time of burning per specimen after either flame application should not be greater than 10 seconds, and total burning time for the 10 flame applications for each set of 5 specimens should not be greater than 50 seconds.

## Chapter 5: Results and Discussion

In all the properties considered, pre-exposure measurement results were used to characterize the laminate materials. The laminate material data sheet values are listed in Appendix I. In the following subsections, the effects of laminate material constituents (such as curing agent, fillers, and flame retardant) in relationship to changes in the material properties due to lead-free soldering exposures are discussed.

### 5.1 Glass transition temperature ( $T_g$ )

The pre and post-exposure  $T_g$  measurement results were grouped by material (e.g., A, B, C1) as shown in Figure 25. Under each material group the results of four sets of data are represented. The first set of data points shown in each group corresponds to the results of control samples, the second set to 3X reflowed samples, the third set to 6X reflowed samples, and the fourth set to the samples that were exposed to a combination of 2X reflow and 1X wave soldering cycles. This pattern of data representation is followed in all the properties except time-to-delamination and flammability. The materials that underwent a mean-to-mean variation of greater than 5°C in  $T_g$  after the exposures are highlighted in Figure 25.

The control sample results show to have a similar  $T_g$  range for the laminates, irrespective of the type of curing agent, the type of flame retardant, and the presence of fillers. For example, materials A to E have a  $T_g$  range of 165°C to 180°C even though they differ by the material constituents. The  $T_g$  of a laminate system primarily depends on the type of epoxy (bi, tetra or multi-functional) and its percentage

composition. Higher cross-linking density in the multi-functional epoxy systems compared to their bi-functional counterparts results in a higher  $T_g$ .

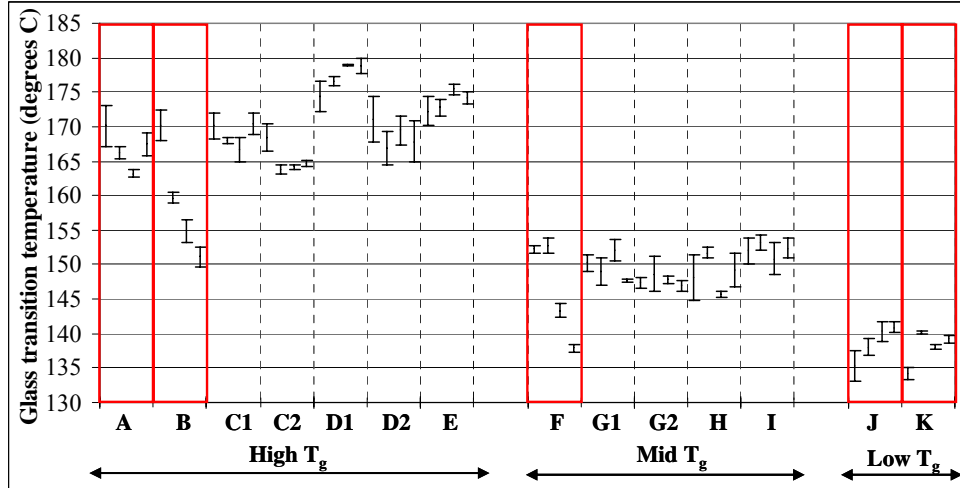


**Figure 25: Effect of lead-free soldering exposures on  $T_g$  of the laminates**

The post-exposure results show that five out of seven high  $T_g$  and four out of five mid  $T_g$  materials have relatively stable  $T_g$  with a variation of less than  $5^\circ\text{C}$ . All of these are phenolic-cured materials. The materials (A, B, F, J and K) that underwent a mean-to-mean variation in  $T_g$  of greater than  $5^\circ\text{C}$  are all DICY-cured. A decrease in  $T_g$  was observed in high and mid  $T_g$  DICY-cured materials, whereas an increase in  $T_g$  was observed in low  $T_g$  DICY-cured materials. The highest variation in  $T_g$  (a reduction of about  $20^\circ\text{C}$  from control) was observed in the high  $T_g$  DICY-cured halogen-free material (B).

The  $T_g$  of laminates was also obtained from the coefficient of thermal expansion measurement plots by TMA. The  $T_g$  comparison between DSC and TMA is shown in Table 7. The difference in  $T_g$  values between DSC and TMA methods is due to the difference in measurement method. In DSC, the midpoint of transition in heat

capacity is taken as  $T_g$ , whereas in TMA the point at which slopes of CTE plot change is taken as  $T_g$ .

**Table 7: The  $T_g$  comparison between DSC and TMA methods**

#	Datasheet	Control		3X Reflow		6X Reflow		2X-R+1X-W	
		DSC	TMA	DSC	TMA	DSC	TMA	DSC	TMA
A	165-175 (DSC)	170.1	172.0	166.3	171.8	163.2	163.7	167.5	159.8
B	165-175 (DSC)	170.3	160.0	159.7	158.0	154.9	154.9	151.1	151.3
C1	165-175 (DSC)	170.1	167.6	168.0	163.8	166.6	163.9	170.4	165.8
C2	165-175 (DSC)	168.5	167.1	163.8	166.3	164.2	168.5	164.7	161.1
D1	173-183 (DSC)	174.4	152.9	176.6	162.0	178.9	163.8	178.8	165.3
D2	170-175 (DSC)	171.1	163.8	166.9	161.8	169.5	163.9	167.8	158.6
E	170-180 (TMA)	172.2	170.3	172.8	167.4	175.4	165.7	174.1	165.4
F	145-155 (DSC)	152.2	157.1	152.8	151.5	143.3	147.7	137.9	145.4
G1	150-160 (DSC)	150.3	156.3	149.0	149.8	152.1	152.1	147.7	153.0
G2	145-155 (DSC)	147.4	156.0	148.6	153.4	147.8	151.7	146.9	148.7
H	135-145 (DSC)	148.1	149.2	151.7	146.9	145.7	148.6	149.2	146.8
I	140-150 (TMA)	152.0	138.1	153.2	138.1	150.8	134.5	152.4	137.2
J	135-145 (TMA)	135.4	137.2	138.0	144.2	140.3	141.2	140.9	137.0
K	175-185 (DMA)	134.2	136.2	140.2	139.5	138.0	139.8	139.2	136.7

## 5.2 Coefficient of thermal expansion (CTE)

The out-of-plane CTE (below and above  $T_g$ ) measurement results are shown in Figure 26. The materials that underwent a mean-to-mean variation of greater than 15% in (above  $T_g$ ) CTE after the exposures are highlighted in the figure.

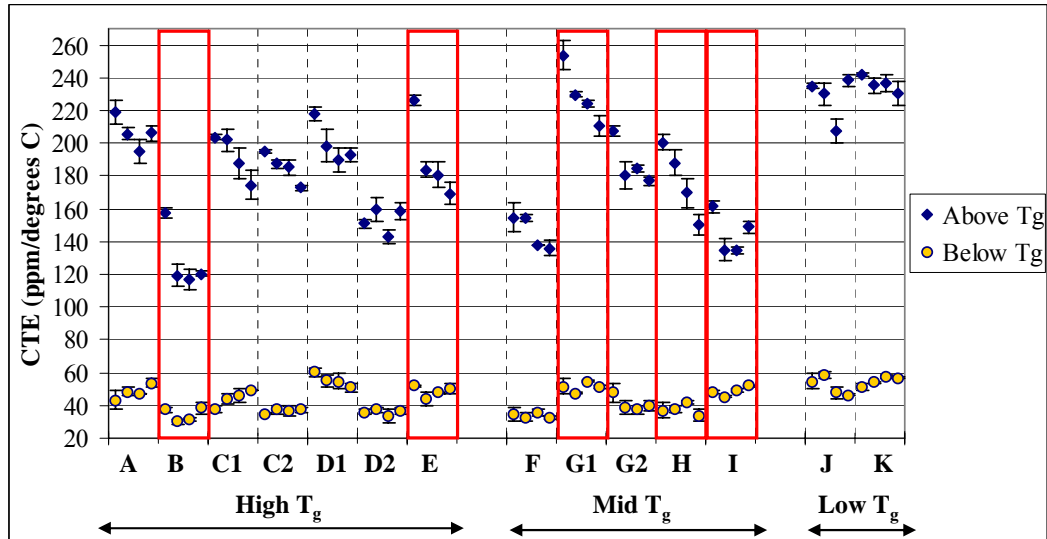


**Figure 26: Effect of lead-free soldering exposures on out-of-plane CTE of the laminates**

The control results show that high  $T_g$  material (A) has lower CTE compared to a low  $T_g$  material (J) with similar constituents (DICY-cured with halogenated flame retardant). This is because of the higher cross-linking density in the epoxy resin system of high  $T_g$  materials that resists the thermal expansion of the laminate. DICY and phenolic-cured materials have similar CTE range (A vs. C1). Filled materials have lower CTE values compared to unfilled materials (C2 vs. C1, D2 vs. D1, G2 vs. G1), as fillers replace the epoxy in filled materials. Halogen-free materials have lower CTE values than halogenated materials (B vs. A, I vs. H). This could be because of the combined effect of presence of fillers and material chemistry of halogen-free laminates that typically result in lower CTE values than the halogenated laminates [10].

The post-exposure results show a reduction of out-of-plane CTE in most of the materials, with a highest reduction of approximately 25% observed in the above  $T_g$

CTE of material B. The reduction in CTE could be due to further curing of the resin system, resulting in an increase in the cross-linking density.

The control in-plane (warp and fill) CTE measurements were performed on all the materials and the results are shown in Table 8. The post-exposure measurements were performed on six materials A, B, C1, F, G2 and J (shown in Table 9 and Table 10) as similar CTE values were observed in all the materials irrespective of the type of curing agent, flame retardant and presence of fillers. Post-exposure in-plane CTE results did not show noticeable variation.

**Table 8: Control in-plane (warp and fill) CTE measurement results**

Supplier	Material ID	Material classification			Warp		Fill	
		Curing agent	Fillers	Halogen-free	Below T <sub>g</sub>	Above T <sub>g</sub>	Below T <sub>g</sub>	Above T <sub>g</sub>
I	A	DICY	No	No	11.8±0.2	1.1±0.1	15.4±0.5	7.9±1.4
I	B	DICY	Yes	Yes	12.2±0.7	2.7±1.0	14.8±0.3	9.8±0.5
I	C1	Phenolic	No	No	13.4±1.5	4.3±1.1	16.3±0.5	12.2±0.7
I	C2	Phenolic	Yes	No	12.6±0.5	3.9±0.7	14.6±0.5	11.6±0.5
II	D1	Phenolic	No	No	14.7±2.3	3.3±0.6	16.9±1.5	11.3±1.0
II	D2	Phenolic	Yes	No	13.4±0.9	3.9±1.1	18.9±1.4	13.4±0.8
II	E	Phenolic	Yes	Yes	15.2±1.5	3.2±0.6	16.2±0.8	9.5±0.5
I	F	DICY	Yes	Yes	12.1±0.8	4.9±1.0	16.8±1.9	10.6±0.5
I	G1	Phenolic	No	No	13.1±0.7	2.0±0.2	15.2±0.8	10.4±1.2
I	G2	Phenolic	Yes	No	15.2±2.7	3.5±2.5	14.6±0.4	10.9±0.8
II	H	Phenolic	Yes	No	14.1±0.8	4.2±0.2	18.8±1.2	13.5±2.4
II	I	Phenolic	Yes	Yes	17.9±1.2	3.1±0.9	17.8±1.2	7.9±0.3
I	J	DICY	No	No	12.1±0.5	2.2±1.1	14.9±0.5	10.2±1.8
I	K	DICY	Yes	No	13.0±1.1	2.8±0.4	15.7±0.3	10.8±0.1

**Table 9: Post exposure in-plane (warp) CTE measurement results**

Material ID	Control		3X Reflow		6X Reflow		2X R+ 1X wave	
	Below T <sub>g</sub>	Above T <sub>g</sub>	Below T <sub>g</sub>	Above T <sub>g</sub>	Below T <sub>g</sub>	Above T <sub>g</sub>	Below T <sub>g</sub>	Above T <sub>g</sub>
A	11.8±0.2	1.1±0.1	14.1±0.1	1.4±0.2	13.7±1.5	0.9±0.1	15.3±1.3	1.8±0.5
B	12.2±0.7	2.7±1.0	13.5±1.1	3.4±0.8	12.9±3.1	2.1±0.6	14.8±2.7	3.2±1.5
C1	13.4±1.5	4.3±1.1	15.7±1.1	3.5±0.9	13.6±2.7	4.5±1.7	15.2±1.9	3.8±0.9
F	12.1±0.8	4.9±1.0	15.9±1.8	2.2±1.9	13.6±2.4	1.8±0.7	11.2±1.5	2.4±0.5
G2	15.2±2.7	3.5±2.5	13.3±1.3	4.2±1.1	16.3±2.1	3.8±0.9	12.3±0.8	2.3±1.1
J	12.1±0.5	2.2±1.1	14.9±2.3	4.9±2.8	13.6±1.7	2.6±1.3	12.7±1.9	4.5±2.1

**Table 10: Post exposure in-plane (fill) CTE measurement results**

Material ID	Control		3X Reflow		6X Reflow		2X R+ 1X wave	
	Below T <sub>g</sub>	Above T <sub>g</sub>	Below T <sub>g</sub>	Above T <sub>g</sub>	Below T <sub>g</sub>	Above T <sub>g</sub>	Below T <sub>g</sub>	Above T <sub>g</sub>
A	15.4±0.5	7.9±1.4	14.2±1.1	9.1±0.7	16.3±1.6	8.7±0.7	15.9±1.1	8.6±0.4
B	14.8±0.3	9.8±0.5	16.8±1.2	8.6±1.3	15.1±0.9	9.1±1.4	15.2±0.4	8.4±0.9
C1	16.3±0.5	12.2±0.7	15.7±0.2	11.8±0.2	15.1±1.6	10.6±0.9	15.3±1.2	11.1±1.0
F	16.8±1.9	10.6±0.5	15.1±0.8	9.8±0.3	15.9±1.1	9.1±1.5	16.7±0.7	11.6±0.2
G2	14.6±0.4	10.9±0.8	15.7±1.5	10.1±1.2	13.1±0.9	8.8±0.8	15.1±1.0	9.9±1.1
J	14.9±0.5	10.2±1.8	13.1±1.2	9.1±0.7	14.1±1.9	10.1±1.5	16.8±1.4	11.2±0.5

### 5.3 Decomposition temperature (T<sub>d</sub>)

The decomposition temperature measurement results corresponding to 2% and 5% weight loss are plotted in Figure 27. Lead-free soldering exposures did not show noticeable variation in T<sub>d</sub> (>10°C), and hence no materials are highlighted in the figure.

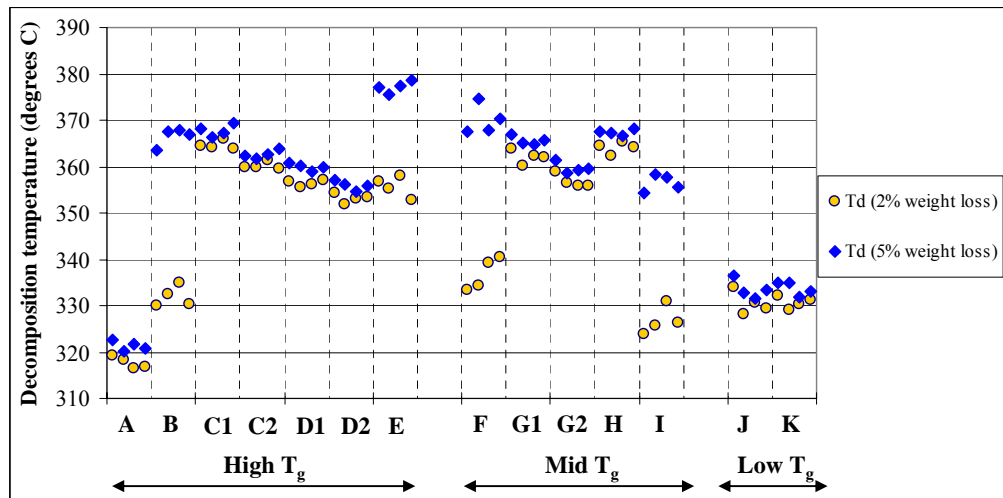


**Figure 27: Effect of lead-free soldering exposures on T<sub>d</sub> of the laminates**

The control measurement results show that low T<sub>g</sub> material (J) has higher T<sub>d</sub> compared to high T<sub>g</sub> material (A) with similar constituents [8]. The comparison of degradation behavior between materials A and J is plotted in Figure 28.

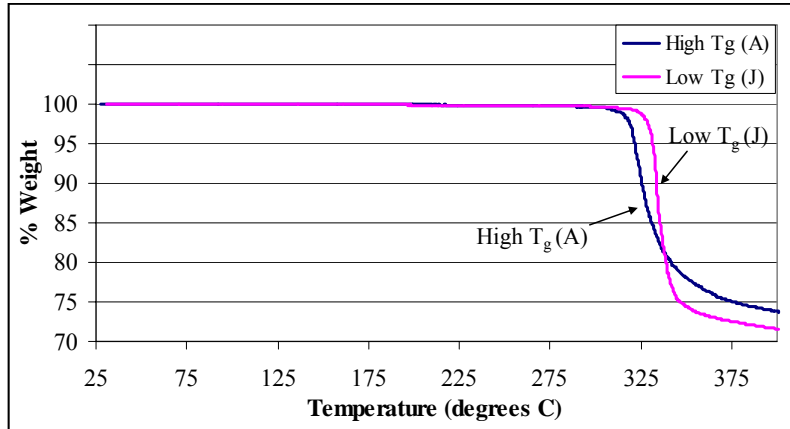


**Figure 28: T<sub>d</sub> comparison between materials A and J**

Amongst the halogenated materials, phenolic-cured materials (G1, C1) have higher T<sub>d</sub> compared to their DICY-cured counterparts (A, J). The lower decomposition temperatures in DICY-cured epoxy systems could be attributed to the presence of linear aliphatic molecular bonds with amine linkages, compared to more thermally stable aromatic bonds with ether linkages of phenolic-cured systems ([10], [15]) These observations are shown in Figure 29 and Figure 30.

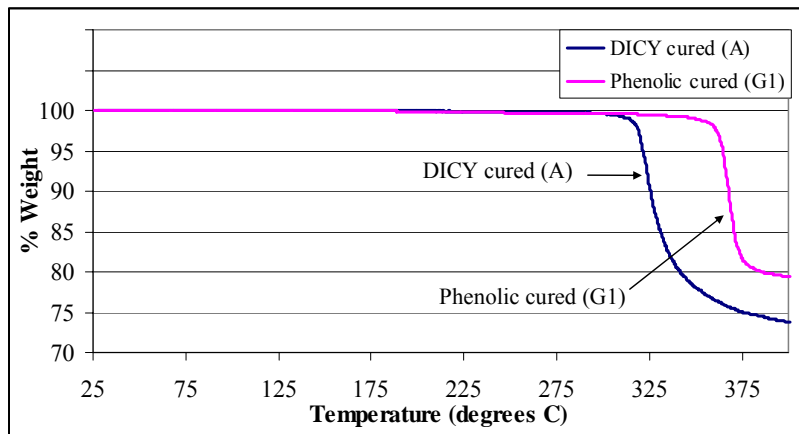


**Figure 29: T<sub>d</sub> comparison between materials A and G1**

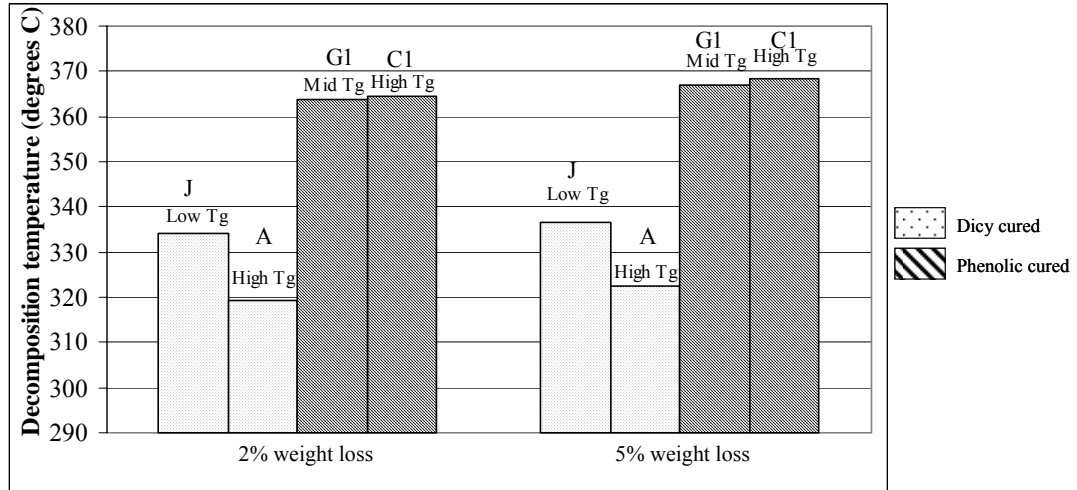


**Figure 30: Effect of type of curing agent on  $T_d$  of the laminates**

Laminates with fillers have lower  $T_d$  compared to their counterparts without fillers (C2 vs. C1, D2 vs. D1, G2 vs. G1). Inorganic fillers such as alumina or silica accelerate the thermal decomposition process by lowering the activation energy required for decomposition, thereby acting as catalysts ([33], [34], [35]). These observations are shown in Figure 31 and Figure 32.

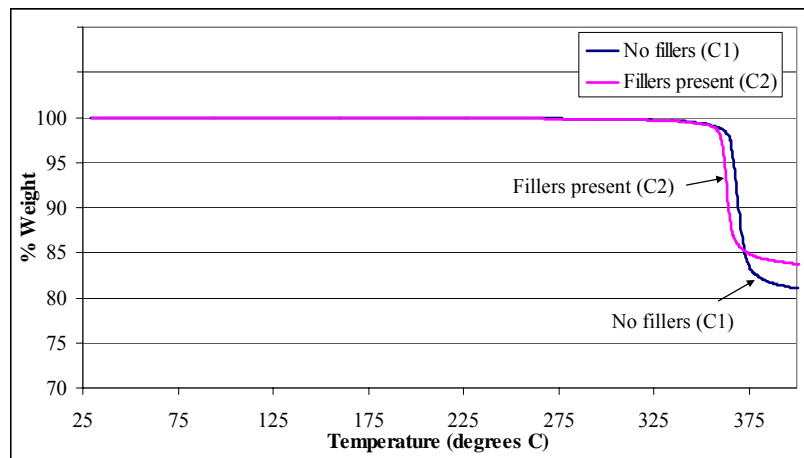


**Figure 31:  $T_d$  comparison between materials C1 and C2**

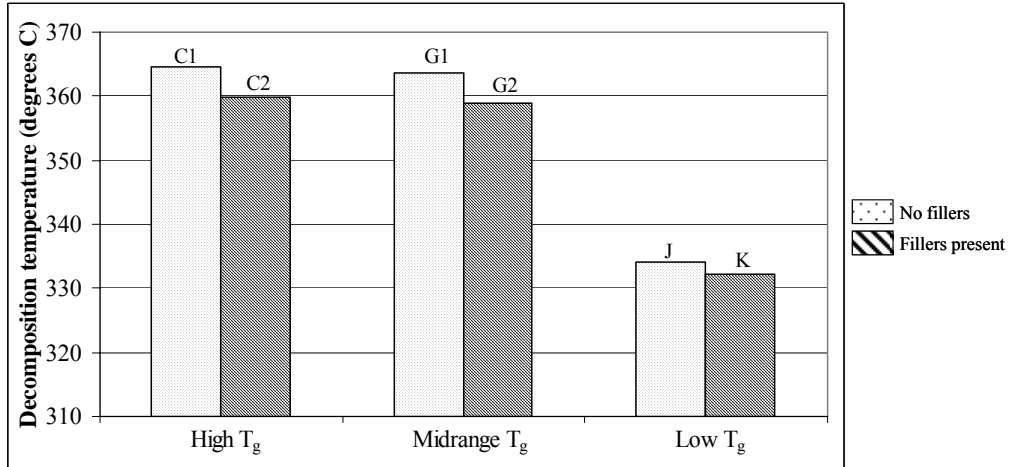


**Figure 32: Effect of presence of fillers on T<sub>d</sub> of the laminates**

Halogen-free material that is DICY-cured (B) could withstand higher temperatures before 2% and 5% weight degradation compared to the halogenated DICY-cured material (A) (shown in Figure 33). On the contrary, halogen-free material that is phenolic-cured (I) has lower T<sub>d</sub> compared to its halogenated counterpart (H) (shown in Figure 34). Irrespective of the type of curing agent, halogenated resin systems (A, H) underwent degradation from 2% to 5% within a narrow temperature range, which was not observed in halogen-free systems (B, I) (shown in Figure 34).

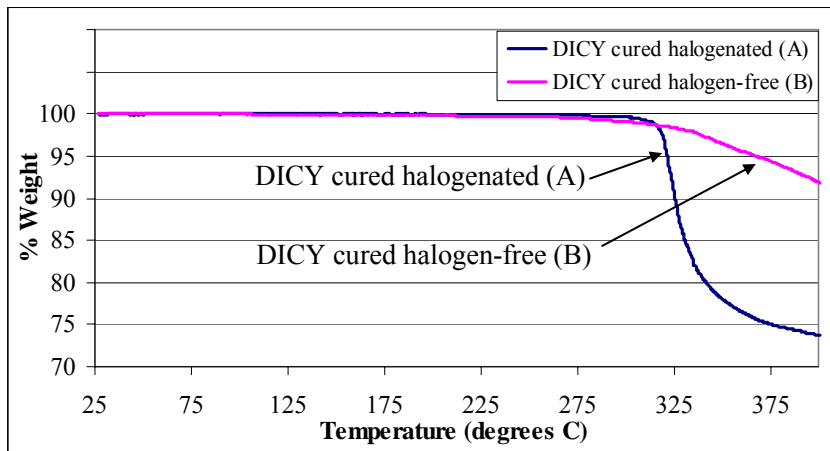


**Figure 33: T<sub>d</sub> comparison between materials A and B**

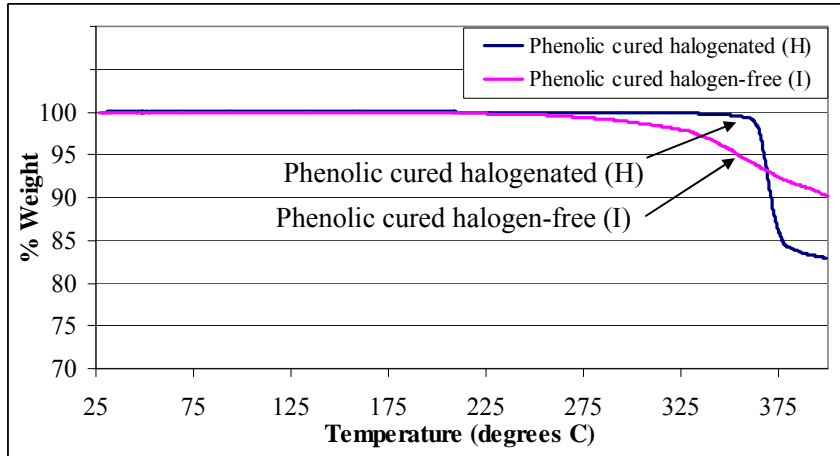


**Figure 34: T<sub>d</sub> comparison between materials H and I**

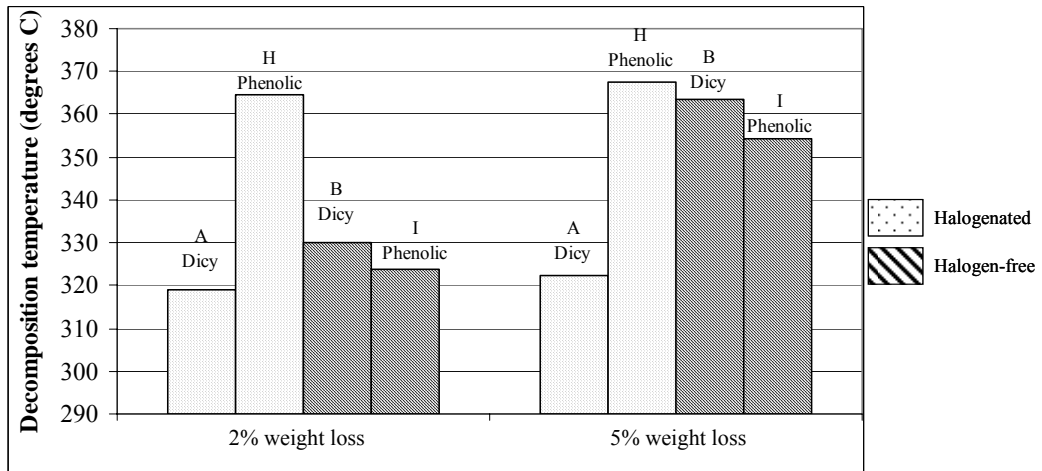


**Figure 35: Effect of type of flame retardant on T<sub>d</sub> of the laminates**

The post-exposure results show a maximum variation of 7°C in decomposition temperature of the laminates. The effect of material constituents such as curing agents, fillers, and flame retardants on the decomposition temperatures for the control samples remained the same after the exposures.

#### 5.4 Time-to-delamination (T-260)

Time-to-delamination was measured for fabricated boards on a subset of materials i.e., A, B, C1, C2, G1, and J and the results are shown in Figure 36. The order of data representation under each material is the same as that of T<sub>g</sub> results.

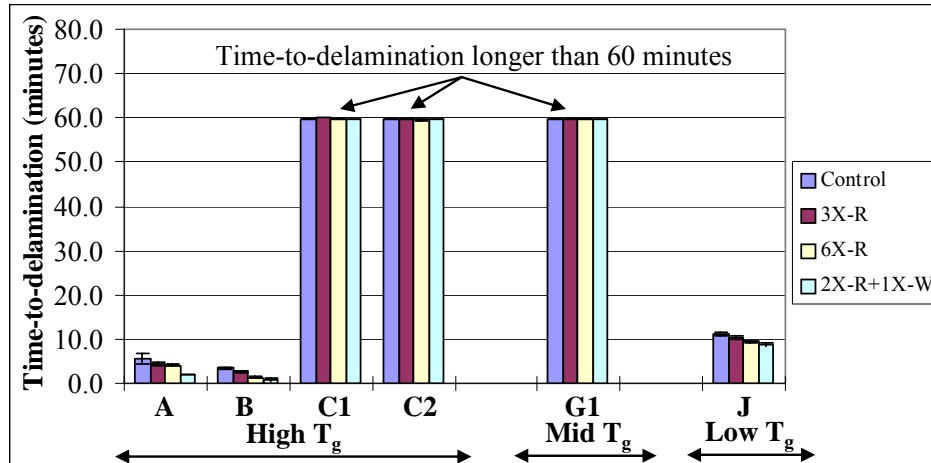


**Figure 36: Effect of lead-free soldering exposures on T-260 of the laminates**

The control results show that three materials A, B and J delaminated within 20 minutes whereas materials C1, C2 and G1 did not delaminate for 60 minutes. Material J has higher T-260 than that of A and B. Thus, DICY-cured materials have lower time-to-delamination compared to phenolic-cured materials irrespective of their T<sub>g</sub>. Low T<sub>g</sub> DICY-cured materials have higher T-260 compared to their high T<sub>g</sub> counterparts. The effect of type of flame retardant and presence of fillers is not as prominent as that of curing agent.

Lead-free soldering exposures tend to lower the time-to-delamination of materials A, B, and J all of which are DICY-cured materials. Materials C1, C2 and G1 which are phenolic-cured did not delaminate below 60 minutes even after exposures.

## 5.5 Water absorption

The pre and post-exposure water absorption measurement results are shown in Figure 37. Average and the range of results from the average of three measurements are plotted. Materials with a variation of greater than 25% in water absorption from control are shown within separate boxes in Figure 37.

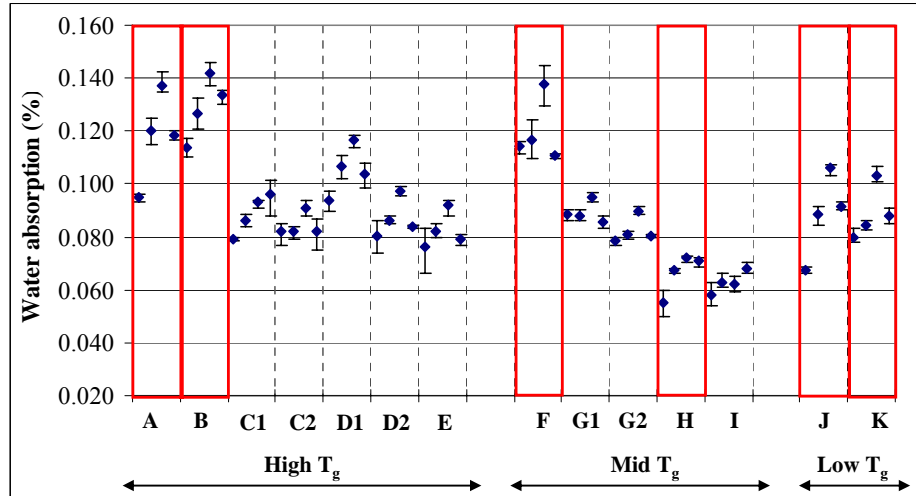


**Figure 37: Effect of lead-free soldering exposures on water absorption**

The control sample results show that high  $T_g$  materials (A, B) have higher water absorption compared to low  $T_g$  materials (J, K) with similar constituents. This could be attributed to the availability of higher free volume due to higher cross-linking density in the high  $T_g$  materials compared to low  $T_g$  materials [36]. DICY-cured epoxy systems are more hygroscopic compared to phenolic-cured systems (A vs. C1, F vs. I) because of the presence of highly polar bonds in the former compared to the later [15]. The effect of presence of fillers and type of flame retardant is not as prominent as that of type of curing agent.

The post-exposure results showed an increase in water absorption due to lead-free soldering exposures for most of the materials. The material type with highest increase in water absorption value (55%) after 6X reflow exposure is a low  $T_g$  DICY-cured halogenated material (J).

## 5.6 Flammability

The pre and post-exposure flammability measurement results are shown in Figure 38 and Figure 39. Total burning time for the 10 flame applications for each set of 5

specimens is plotted in Figure 38, whereas average burning time and one standard deviation is plotted in Figure 39. The UL 94 V-0 flammability criteria i.e., total burning time for the 10 flame applications for each set of 5 specimens should not be greater than 50 seconds, is shown in Figure 38.

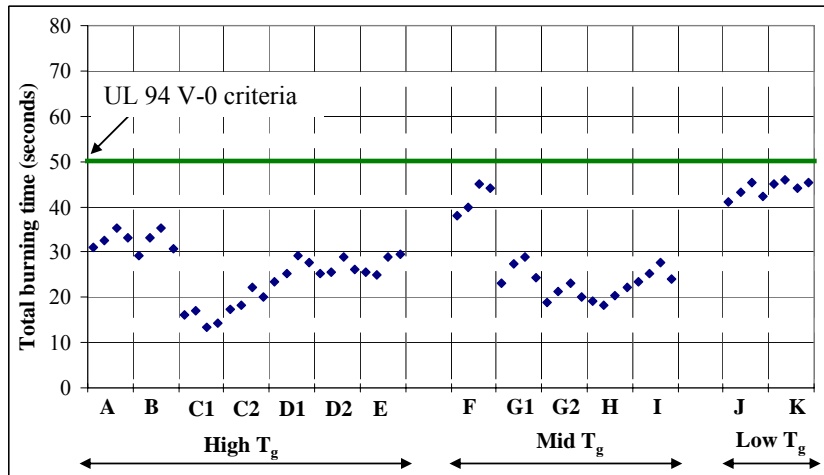


**Figure 38: Effect of lead-free soldering exposures on flammability of the laminates (total burning time)**

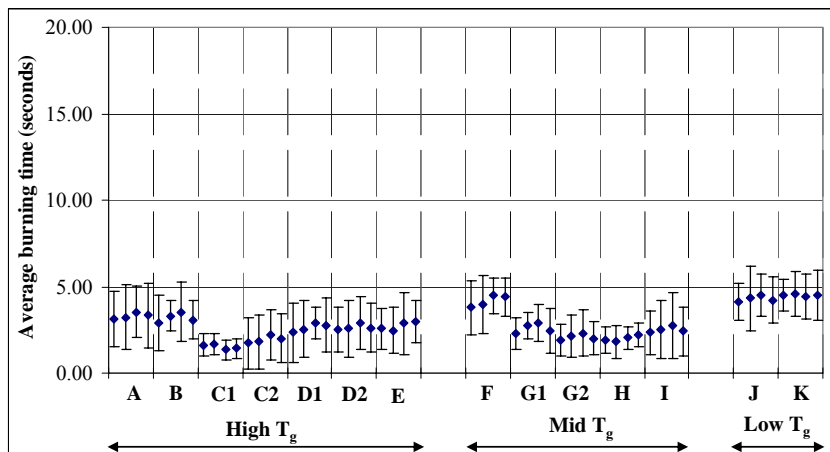


**Figure 39: Effect of lead-free soldering exposures on flammability of the laminates (Average burning time)**

The control sample results show that UL 94 V-0 flammability criteria are satisfied by all the samples. The effect of material constituents on the flammability of the laminates is more prominent in Figure 38 compared to Figure 39. Low  $T_g$  material (J)

has higher flammability compared to high  $T_g$  material (A) with similar constituents. DICY-cured materials (A, B, F, J, K) have higher burning times compared to phenolic-cured systems irrespective of  $T_g$ , type of flame retardant and presence of fillers. This could be because of the highly aromatic structure of phenolic-cured systems that can produce a substantial amount of char which forms a boundary layer between the flame front and the combustible material reducing the flame propagation [31]. Also, the flammable mixture of phenolic-cured systems could still contain higher energy bonds compared to that of DICY-cured systems. The effects of presence of fillers and type of flame retardant are not as prominent as that of the curing agent.

The post-exposure measurement results show that samples still meet UL 94 V-0 flammability criteria after lead-free soldering exposures with a common trend of increase in combustion times observed in most of the materials.

## **Chapter 6: Analysis of Results**

The high temperature exposures associated with lead-free soldering resulted in a noticeable variation in the laminate material properties. The exposures could have possibly resulted in the cleavage of bonds at the chain ends of the epoxy system leading to an ‘enhanced-cure’ structure; or resulted in the cleavage of bonds in polymer backbone leading to a ‘degraded’ structure. The former mechanism results in an increase in the cross-linking density of the epoxy matrix whereas the later results in a change in the material structure due to loss of certain functional groups [37], both of which can potentially change the material properties of laminates. Fourier transform infrared spectroscopy (FTIR) analysis was performed to verify the possible degradation in the epoxy structure, and combinatorial analysis of material properties is performed to verify the enhanced-cure structure.

### **6.1 Fourier transform infrared (FTIR) spectroscopy analysis**

#### **6.1.1 Introduction**

Fourier transform infrared (FTIR) spectroscopy is a tool that provides structural information about the presence of certain functional groups in a material. Electromagnetic radiation in the infrared (IR) region is directed at the sample which absorbs (or transmits) the infrared radiation at different frequencies and produces a unique spectra based on the frequencies at which it absorbs (or transmits) IR, and the intensity of the absorption (or transmission). The absorption (or transmission) is shown as a peak in the FTIR spectrum. The wave number corresponding to the peak

is an indication of the energy absorbed (or transmitted). Each molecule has its own distinct quantized vibrational energy level, and hence the wave number which are related by the following expression.

$$\Delta E_{\text{vib}} = hc \bar{\nu}, \text{ h-Planck's constant; c- speed of light, } \bar{\nu} - \text{wave number}$$

Each wave number depends on several factors such as mass of the atoms, force constants of the bonds, and geometry of the molecules. The absorbed energy of infrared radiation is converted into atomic bond vibrations. Different types of molecular bending movements are shown in Figure 40.

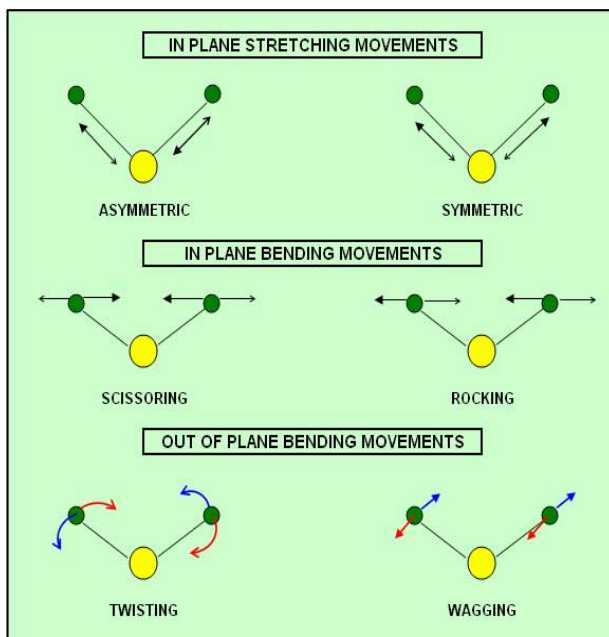


**Figure 40: Common molecular bending movements [38]**

The atomic vibrations are classified as either stretching or bending. Stretching vibrations are categorized as being either symmetrical (movement in the same direction) or asymmetrical (movement in opposite directions). Bending vibrations are classified as scissoring, rocking, twisting, or wagging.

### 6.1.2 Analysis

FTIR analysis is performed on the laminates to identify the key functional groups in the material systems and investigate their possible changes due to lead-free soldering exposures, and correlate the compositional changes to the variation in material properties. Samples from control and 6X reflowed lots of materials B and H that underwent significant variation in the properties were selected for the analysis.



Mattson FTIR spectrometer with Galaxy Microscope attachment was used for the analysis. A small piece of the material was taken from the sample using a stainless steel scalpel and mounted on an IR-reflective brass plate. IR beam was passed through the sample and then reflected off of the brass plate and passed back through the sample where it was detected and analyzed. Each sample was scanned 32 times with  $4\text{ cm}^{-1}$  resolution to obtain the spectrum.

FTIR library was prepared from the literature with typical wave numbers corresponding to the functional groups present in epoxy systems and is shown in Table 11. Due to the nature of various types of atomic vibrations, a functional group appears with different wave numbers in the library. From the knowledge of basic chemical structures present in the epoxy systems, the functional groups present in the laminate materials were identified. The wave numbers corresponding to the functional groups are listed in Figure 41 based on the prepared FTIR library.

**Table 11: Typical functional groups and wave numbers present in epoxy systems**

Absorption (cm <sup>-1</sup> )	Functional groups	Origin	Reference
3500-3400	-OH or -NH <sub>2</sub>	-OH from opening of epoxy ring and -NH <sub>2</sub> from DICY curing agent	[39]
3350-3200	-NH <sub>2</sub> and -NH	From BAP, TAM (phosphorus containing-amine curing agents) cured epoxy systems	[17]
3410	phenyl-OH	From DHPDOPO (phosphorous based flame retardant)	[40]
3323	phenyl-OH	From BHPPO (phosphorous based flame retardant)	[41]
2900	-CH	From epoxy resin	[42]
2980-2850	-CH	From WSR-HPPE (epoxy resin with phosphorus flame retardant)	[43]
2384	P-H stretch	From DOPO (monomer for DHPDOPO-phosphorous based flame retardant)	[40]
2180	-C≡N (Nitrile)	From DICY-cured epoxy	[44]
1740	-C=O (Carbonyl)	From DICY-cured epoxy	[44]
1728, 1721	-C=O	From organo phosphate esters, (phosphorus containing copoly esters (PET-co-PEPPs))	[18]
1723	-C=O	From WSR-HPPE (epoxy resin with phosphorus based flame retardant)	[43]
1660	-C=N (Imine stretch)	From DICY-cured epoxy	[44]
1650	-C=N	From DICY-cured epoxy	[44]
1640	-C=O	From BAP, TAM (phosphorus containing-amine curing agents) cured epoxy systems	[17]
1630, 1565	-N-H (Amine bend)	From DICY-cured epoxy	[44]
1604, 1492	Aromatic C-C	From BHPPO-containing epoxy resin (phosphorus based flame retardant system)	[41]
1594	Aromatic C-C	From DDS curing agent	[39]
1591	phenyl-P	From DHPDOPO (phosphorous based flame retardant)	[40]
1591, 1298, 715	phenyl-NH <sub>2</sub>	From epoxy resin	[42]
1509	Aromatic C-C	From DGEBA (unbrominated epoxy resin)	[39]
1506	Aromatic C-C	From epoxy resin	[42]
1479	Aromatic C-C	From BHPPO (phosphorus containing flame retardant)	[41]
1466	Aromatic C-C	From DGEBTBA (brominated epoxy)	[39]
1461, 1350	phenyl-P	From BGPPPO (phenyl phosphine) resin with DDS curing agent	[45]
1457	phenyl-P	From DGEBA with DHPDOPO and BPA (phosphorus containing epoxy system)	[40]
1363	-CH <sub>3</sub>	From DGEBA with DHPDOPO and BPA (phosphorus containing epoxy system)	[40]
1296	P=O	From WSR-HPPE (epoxy resin with phosphorus flame retardant)	[43]

Absorption (cm <sup>-1</sup> )	Functional groups	Origin	Reference
1289	P=O	From BPHPPPO-containing epoxy resin (phosphorus based flame retardant epoxy system)	[41]
1283	P=O	From BGPPPO (phenyl phosphine) resin with DDS curing agent	[45]
1276	P=O	From BPHPPPO (phosphorus based flame retardant)	[41]
1276	S=O	From DDS curing agent	[39]
1272	phenyl-O	From DGEBTBA (brominated epoxy)	[39]
1263, 995	phenyl-C-P	From BPHPPPO-containing epoxy resin (phosphorus based flame retardant epoxy system)	[41]
1249, 1228	P=O	From organo phosphate esters (phosphorus containing copoly esters (PET-co-PEPPs))	[18]
1246	phenyl-O	From DGEBA	[39]
1246	phenyl-O	From DGEBA with DHPDOPO and BPA (phosphorus containing epoxy system)	[40]
1234, 979	phenyl-O-P stretch	From BPHPPPO (phosphorus based flame retardant)	[41]
1236, 817	-C-O-C-	From epoxy resin	[42]
1195	P=O	From DHPDOPO flame retardant	[40]
1184	P=O	From DGEBA with DHPDOPO and BPA (phosphorus containing epoxy system)	[40]
1176, 1131	P-O-C	From organo phosphate esters (phosphorus containing copoly esters (PET-co-PEPPs))	[18]
1066	phenyl-Br	From DGEBTBA (brominated epoxy)	[39]
1036	phenyl-O-C	From DGEBA (unbrominated epoxy)	[39]
1034	P-O-C	From WSR-HPPE (phosphorus based flame retardant epoxy system)	[43]
1001	phenyl-O-C	DGEBTBA (brominated epoxy)	[39]
970	P-O	From organo-phosphate esters (phosphorus containing copoly esters (PET-co-PEPPs))	[18]
926, 755	phenyl-O-P	From DHPDOPO flame retardant	[40]
915	CH <sub>2</sub> -O-CH <sub>2</sub> (epoxide ring)	From epoxy resin monomer	[44]
915	CH <sub>2</sub> -O-CH <sub>2</sub> (epoxide ring)	From DGEBA with DHPDOPO and BPA (phosphorus containing epoxy system)	[40]
909	CH <sub>2</sub> -O-CH <sub>2</sub>	From BPHPPPO-containing epoxy resin (phosphorus based flame retardant system)	[41]
739	phenyl-H	DGEBTBA (brominated epoxy)	[39]

1. Resin (DGEBA)	
Functional groups	Absorption (cm <sup>-1</sup> )
-C-OH	3500-3400
-C-H	3000-2850
	1600-1450
phenyl-O-C	1040-1000
	915-905

2. Curing agent			
DICY curing agent		Phenolic curing agent	
Functional groups	Absorption (cm <sup>-1</sup> )	Functional groups	Absorption (cm <sup>-1</sup> )
-NH-	3350-3200	Functional groups listed in 1 (Resin) also exist in phenolic curing agent	
-C=N-	1650		

3. Flame retardant (FR)			
Bromine based FR		Phosphorus based FR	
Functional groups	Absorption (cm <sup>-1</sup> )	Functional groups	Absorption (cm <sup>-1</sup> )
phenyl-Br	1066	phenyl-P	1590, 1460, 1350
		P=O	1300-1180

**Figure 41: Typical functional groups present in the epoxy laminate systems**

Complex molecular structure of the laminates combined with the overlap of bond energies made it difficult to interpret the spectra by locating the exact wave numbers corresponding to the functional groups. The peaks corresponding to key functional groups were identified in the FTIR spectra of material H (control sample) (shown in Figure 42). Material H is a mid  $T_g$  phenolic-cured brominated flame retardant system with fillers and hence the following functional groups exist in the material: OH: 3500–3400 cm<sup>-1</sup>, CH: 3000–2850 cm<sup>-1</sup>, Benzene ring: 1600–1450 cm<sup>-1</sup>, Phenyl-Br: 1066 cm<sup>-1</sup>. The spectra corresponding to the control and 6X reflowed samples of

material H is shown in Figure 43 for illustration. The spectra of material B is shown in Appendix II.

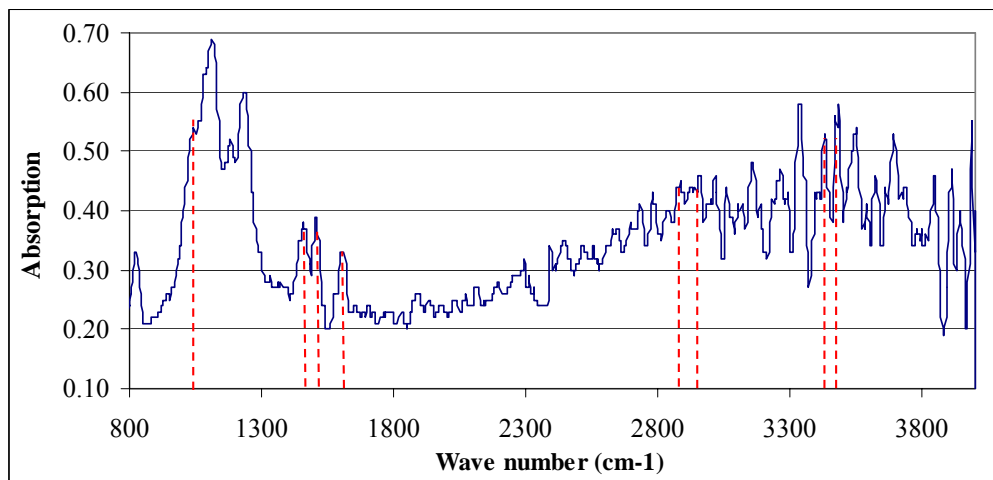


**Figure 42: FTIR spectrum of control sample with functional groups identified (material H)**

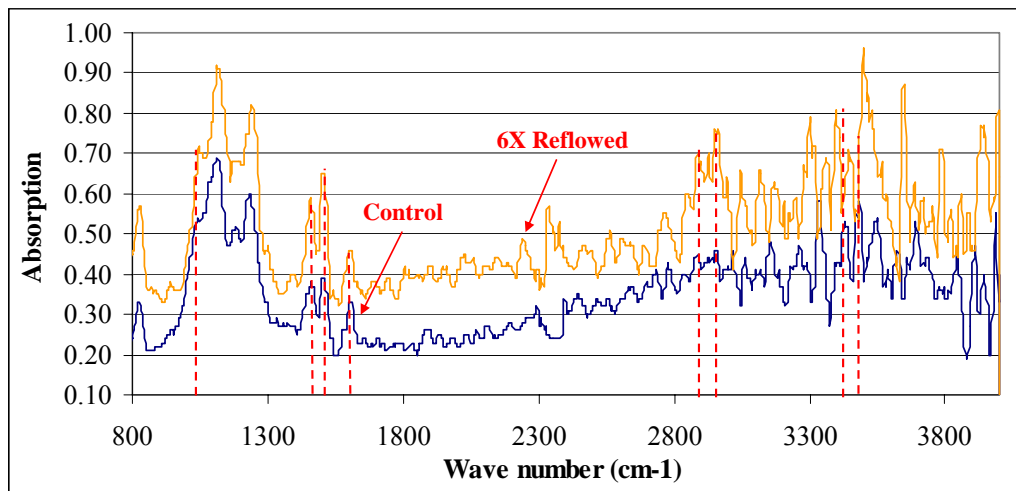


**Figure 43: FTIR spectra of a control and 6X reflowed sample (material H)**

FTIR results did not show noticeable change in the wave numbers corresponding to the functional groups between control and 6X reflowed samples (shape of the spectrum is retained). This indicates that the variation in material properties could possibly be attributed to an increase in cross-linking of the resin system than to the degradation of the polymer network. The results of decomposition temperature

measurements also compliment this as no noticeable variation in  $T_d$  of the materials was observed due to lead-free soldering exposures.

## 6.2 Combinatorial property analysis

A combinatorial property analysis to investigate the underlying mechanisms for the variations in material properties is illustrated for materials B and H. B is a high  $T_g$  DICY-cured halogen-free material with fillers, whereas H is a mid  $T_g$  phenolic-cured halogenated material with fillers. The illustration is focused on the material properties listed in Table 12 and the magnitude of variation shown in the table is between the results of control and 6X reflowed samples. The analysis is aimed at correlating the variations in material properties to the assumed enhanced-cure structure.

**Table 12: Summary of variations in properties for materials B and H**

Property	Material ID	Observed variation	Magnitude of variation
Glass transition temperature ( $T_g$ )	B	Decrease	>5°C
Coefficient of thermal expansion (CTE, out-of-plane)	B, H	Decrease	>15%
Water absorption	B, H	Increase	>25%

The reduction of CTE observed in the 6X reflowed samples of materials B and H could be attributed to the increased cross-linking density of the epoxy resin in the assumed enhanced-cure structure. Water absorption in the epoxy matrix occurs due to the availability of free-volume in the laminate and the affinity of water molecules to the polar sites present in the polymer ([36], [46], [47]). An increase in cross-linking density of the resin system enhances the free-volume of the polymer structure making the laminates more hydrophilic, resulting in an increase in water absorption ([36],

[48], [49], [50]). This could be the cause of increase in water absorption after exposures observed in materials B and H.

The  $T_g$  of a polymer is dependent on several parameters such as molecular weight, degree of cross-linking, and entrapped plasticizers [51]. Water typically acts as a plasticizer in the epoxy systems, resulting in a reversible reduction of  $T_g$  ([52], [53], [54], [55]). As discussed earlier, the laminates exposed to soldering conditions are more susceptible to moisture absorption. A decrease of  $T_g$  observed in material B could be the result of the plasticizing effect of moisture. The samples might have retained the moisture even after the preconditioning (2 hours of baking at 105°C) performed prior to  $T_g$  measurement as per the IPC test method. Material B is a DICY-cured system, and hence has highly polar bonds compared to phenolic-cured material H. Also, B is a high  $T_g$  material having high cross-linking density compared to mid  $T_g$  material H. The combined effect of high polarity and the presence of greater free-volume in the structure could have resulted in a higher moisture absorption in material B, leading to a reduction of  $T_g$ .

To further verify the hypothesis,  $T_g$  of the 6X reflowed samples of material B was measured after baking at 110°C for 24 hours. It was found that the  $T_g$  reduction between control and 6X reflowed samples decreased from 15°C to 8°C, thus proving that the increase in hydrophilic nature of the material results in a degradation of  $T_g$ . The  $T_g$  of material F (mid  $T_g$  DICY-cured halogen-free) was also measured after baking at 110°C for 24 hours, and a decrease in the reduction of  $T_g$  from 9°C to 4°C between control and 6X reflowed samples was observed. These observations are represented in Figure 44. The incomplete recovery of the  $T_g$  after baking suggest a

possibility for a secondary mechanism in the high and mid  $T_g$  DICY-cured halogen-free systems contributing to the reduction of  $T_g$  due to lead-free soldering exposures.

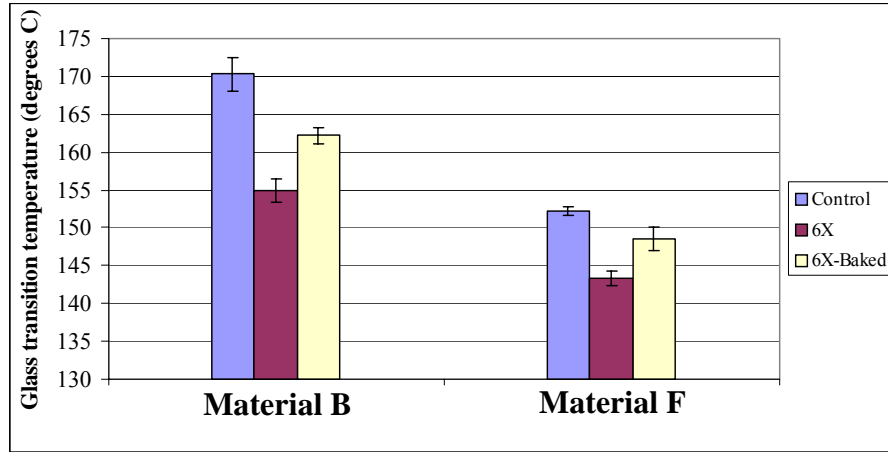


**Figure 44: Effect of baking on the  $T_g$  of laminates**

## Chapter 7: Summary and Conclusions

Selection of PCB laminates compatible with lead-free processes is primarily based on their material properties, and is also impacted by factors such as application environment, cost, reliability, regulatory compliance, material sources, and availability. The laminate properties are determined by the constituents such as type of epoxy, curing agents, fillers, and flame retardants present in the material.

In the materials studied:

- High  $T_g$  laminates have lower out-of-plane CTE and flammability compared to low  $T_g$  materials. Low  $T_g$  laminates, on the other hand, have higher  $T_d$ , T-260 and lower water absorption compared to high  $T_g$  materials with similar constituents.
- Although DICY and phenolic-cured laminates can have similar  $T_g$  and out-of-plane CTE; a higher  $T_d$ , T-260 and lower water absorption, flammability was observed in the phenolic-cured materials compared to similar DICY-cured counterparts.
- The presence of fillers lowers the out-of-plane CTE of the laminates, whereas the  $T_g$ ,  $T_d$ , T-260, water absorption, and flammability does not have a strong dependence on fillers.
- Halogen-free and halogenated materials can have similar  $T_g$ , T-260, water absorption and flammability, whereas lower out-of-plane CTE was observed in halogen-free materials compared to halogenated materials. Also, halogen-

free material that is DICY-cured has higher  $T_d$  compared to the halogenated DICY-cured material. On the contrary, halogen-free material that is phenolic-cured has lower  $T_d$  compared to its halogenated counterpart.

The high temperature exposures associated with lead-free soldering assembly conditions result in variations in the material properties of certain FR-4 laminate material types. The exposures tend to lower the  $T_g$ , out-of-plane CTE, and T-260 of the laminate materials. An increase in water absorption and flammability was observed in most of the laminates due to exposures. The exposures did not affect the laminate materials to an extent of changing their decomposition temperatures ( $T_d$ ). The variation in material properties due to lead-free soldering exposures is attributed to the degree of cross-linking and to the extent of water absorption in the exposed laminates.

## Chapter 8: Contributions

- This is the first published study demonstrating the effects of lead-free soldering exposures on key thermomechanical, physical, and chemical properties of FR-4 laminates. The analysis of characterization provides a guideline for the selection of laminates for appropriate applications.
- The laminate material types that are most affected by lead-free soldering exposures are illustrated.
- Based on the observations, the following recommendations have been made:
  - Laminate manufacturers should conduct in-house qualification tests on the laminates to assess the variations in material properties. Corrective actions should be taken by tailoring the material constituents and/or laminate fabrication process conditions for achieving thermally stable laminates.
  - Electronic product manufacturers should gather the information about material constituents from the laminate suppliers, and consider the extent of variations in material properties due to lead-free soldering exposures before making a decision on the selection of appropriate laminates.

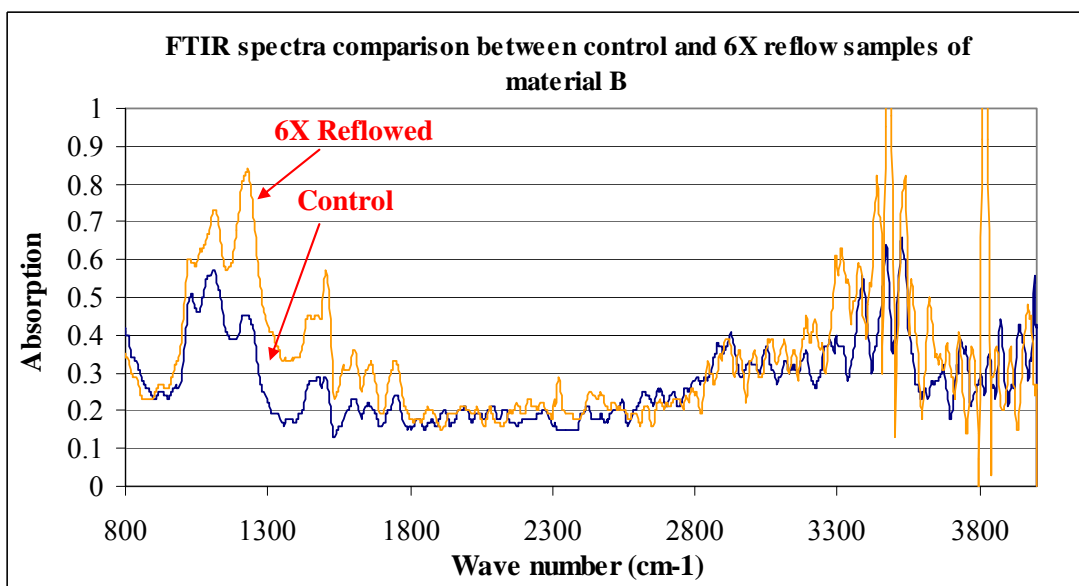
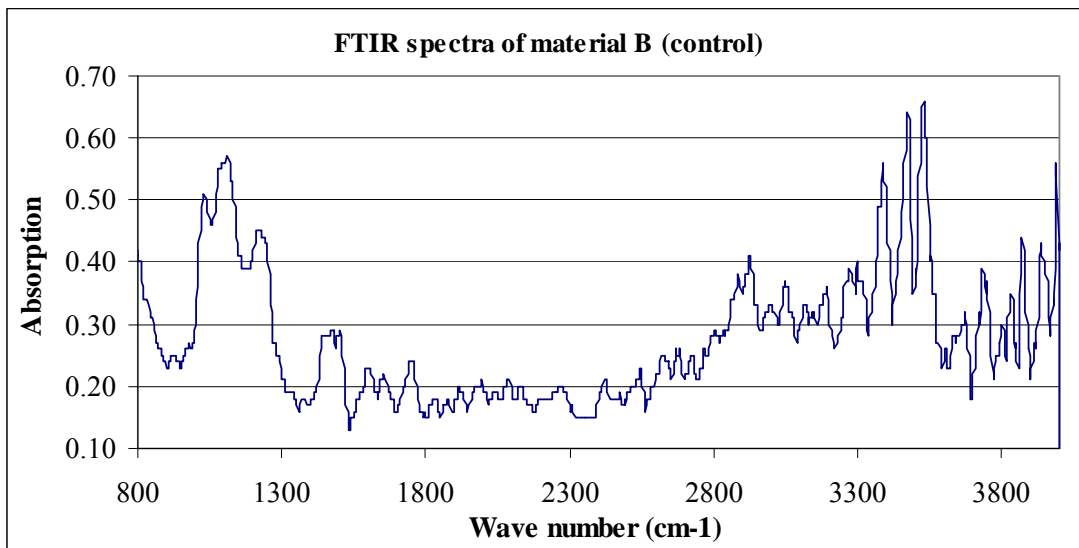
## Appendix I: Datasheet values for the material properties studied

Supplier	#	T <sub>g</sub> (°C)	CTE (ppm/°C) [out-of-plane]		CTE (ppm/°C) [in-plane: warp]		CTE (ppm/°C) [in-plane: fill]	
			Below T <sub>g</sub>	Above T <sub>g</sub>	Below T <sub>g</sub>	Above T <sub>g</sub>	Below T <sub>g</sub>	Above T <sub>g</sub>
I	A	165-175 (DSC)	50-70	200-300	N/A	N/A	N/A	N/A
I	B	165-175 (DSC)	30-50	200-230	N/A	N/A	N/A	N/A
I	C1	165-175 (DSC)	40-60	270-300	N/A	N/A	N/A	N/A
I	C2	165-175 (DSC)	40-60	250-270	N/A	N/A	N/A	N/A
II	D1	173-183 (DSC)	50-60	200-300	12-15	N/A	14-17	N/A
II	D2	170-175 (DSC)	20-30	130-160	12-14	N/A	12-14	N/A
II	E	170-180 (TMA)	40-50	280-310	15-18	N/A	15-18	N/A
I	F	145-155 (DSC)	30-50	200-230	N/A	N/A	N/A	N/A
I	G1	150-160 (DSC)	40-60	270-300	N/A	N/A	N/A	N/A
I	G2	145-155 (DSC)	40-60	250-270	N/A	N/A	N/A	N/A
II	H	135-145 (DSC)	35-45	180-240	12-15	N/A	14-17	N/A
II	I	140-150 (TMA)	40-55	150-220	13-16	N/A	16-19	N/A
I	J	135-145 (TMA)	50-70	250-350	N/A	N/A	N/A	N/A
I	K	175-185 (DMA)	50-70	250-350	N/A	N/A	N/A	N/A

Supplier	#	T <sub>d</sub> (°C)		Water absorption	Flammability
		2% weight loss	5% weight loss		
I	A	N/A	310	0.20-0.30	UL 94 V-0
I	B	N/A	350	0.20-0.30	UL 94 V-0
I	C1	N/A	351	0.20-0.30	UL 94 V-0
I	C2	N/A	351	0.05-0.10	UL 94 V-0
II	D1	N/A	N/A	N/A	UL 94 V-0
II	D2	N/A	N/A	N/A	UL 94 V-0
II	E	N/A	350-370	N/A	UL 94 V-0
I	F	N/A	350	0.20-0.30	UL 94 V-0
I	G1	N/A	350	0.20-0.30	UL 94 V-0
I	G2	N/A	350	0.05-0.10	UL 94 V-0
II	H	N/A	340-360	N/A	UL 94 V-0
II	I	N/A	N/A	N/A	UL 94 V-0
I	J	N/A	325	0.05-0.10	UL 94 V-0
I	K	N/A	350	0.15-0.18	UL 94 V-0

\* The data sheet values are for a specific construction (type of glass weave style, number of glass plies, resin content, and nominal thickness) of the laminate material which is different from that of the laminate materials considered for this study.

## Appendix II: FTIR spectra of control and 6X reflowed samples of material B



## Bibliography

- [1] The European Parliament and the Council of the European Union, “Directive 2002/95/EC on the restriction of the use of certain hazardous substances (RoHS) in electrical and electronic equipment”, *Official Journal of the European Union*, pp. L. 37/19-37/23, February, 2003.
- [2] The European Parliament and the Council of the European Union, “Directive 2002/95/EC on the waste electrical and electronic equipment (WEEE)”, *Official Journal of the European Union*, pp. L. 37/24-37/38, February, 2003.
- [3] Ganesan S., and Pecht M., “Lead-free electronics”, IEEE Press, Wiley-Interscience, A. John Wiley and Sons, Inc., New Jersey, USA, 2006.
- [4] Coombs C., “Printed circuit handbook”, McGraw Hill, fifth edition, 2001.
- [5] Bergum E., “Thermal analysis of base materials through assembly: Can current analytical techniques predict and characterize difference in laminate performance prior to exposure to thermal excursions during assembly?”, *Printed Circuit Design & Manufacture*, September 2003.
- [6] Kelley E., and Bergum E., “Laminate material selection for RoHS assembly, Part 1”, *Printed Circuit Design & Manufacture*, pp. 30-34, November 2006.
- [7] Kelley E., and Bergum E., “Laminate material selection for RoHS assembly, Part 2”, *Printed Circuit Design & Manufacture*, pp. 30-37, December 2006.
- [8] Kelley E., “An assessment of the impact of lead-free assembly processes on base material and PCB reliability,” *Proceedings of IPC APEX Conference*, pp. S16-2-1, 2004.
- [9] Ehrler S., “The compatibility of epoxy-based printed circuit boards with lead-free assembly”, *Circuit World*, vol. 31, no. 4, pp.3-13, 2005.
- [10] Christiansen W., Shirrell D., Aguirre B., and Wilkins J., “Thermal stability of electrical grade laminates based on epoxy resins”, *Proceedings of IPC Printed Circuits EXPO*, Anaheim, CA, pp. S03-1-1-S03-1-7, 2001.

- [11] Valette L., and Wiechmann R., “High-performance substrate from new epoxy resin and enhanced copper foil”, *Circuit World*, vol. 30, no. 4, pp. 20-26, 2004.
- [12] Pecht M., Ardebili H., Shukla A., Hagge J., and Jennings D., “Moisture ingress into organic laminates”, *IEEE Transactions on Components and Packaging Technology*, vol. 22, no. 1, pp. 104-110, March 1999.
- [13] Qi H., Ganesan S., Wu J., and Pecht M., “Effects of printed circuit board materials on lead-free interconnect durability”, *5th International Conference on Polymers and Adhesives in Microelectronics and Photonics*, Wroclaw, Poland, pp. 140-144, October 23-26, 2005.
- [14] Sottos R., Ockers M., and Swindeman M., “Thermoelastic properties of plain weave composites for multilayer circuit board applications”, *Journal of Electronic Packaging, Transactions of the ASME*, vol. 121, no. 1, pp. 37-44, 1999.
- [15] Peng Y., Qi X., and Chrisafides C., “The influence of curing systems on epoxide-based PCB laminate performance”, *Circuit World*, vol. 31, no. 4, pp. 14-20, 2005.
- [16] Camino G., and Costa L., “Performance and mechanisms of fire retardants in polymers—A review”, *Polymer Degradation Stability*, vol. 20, no. 3-4, pp. 271-294, 1988.
- [17] Jain P., Choudhary V., and Varma I., “Flame retarding epoxies with phosphorous”, *Journal of Macromolecular Science-Polymer Reviews*, vol. 42, no. 2, pp. 139-183, 2002.
- [18] Chang, J., Sheen Y., Chang R., and Chang F., “The thermal degradation of phosphorous-containing co polyesters”, *Polymer Degradation and Stability*, vol. 54, no. 2-3, pp. 365-371, 1996.
- [19] Liu W., Varley R., and Simon G., “Understanding the decomposition and fire performance processes in phosphorus and nanomodified high performance epoxy resins and composites”, *Polymer*, vol. 48, no. 8, pp. 2345-2354, 2007.

- [20] Iji M, and Kiuchi Y., "Flame resistant glass-epoxy printed wiring boards with no halogen or phosphorous compounds", *Journal of Materials Science: Materials in Electronics*, vol. 15, pp. 175-182, 2004.
- [21] IPC-4121, "Guidelines for selecting core constructions for multilayer printed wiring board applications", Bannockburn, IL, January 2000.
- [22] IPC/JEDEC J-STD-020D, "Moisture/reflow sensitivity classification for non-hermetic solid state surface mount devices", August 2007.
- [23] IPC-TM-650 2.4.25, "Glass transition temperature and cure factor by DSC", *The Institute for Interconnecting and Packaging Electronic Circuits*, Northbrook, IL, December 1994.
- [24] IPC-TM-650 2.4.24, "Glass transition temperature and z-axis thermal expansion by TMA", *The Institute for Interconnecting and Packaging Electronic Circuits*, Northbrook, IL, December 1994.
- [25] Reinhart J., "Engineering materials handbook", vol. 1, Composites, ASM International, Metals Park, OH, 1987.
- [26] Wu T, Guo Y., and Chen W., "Thermal-mechanical strain characterization for printed wiring boards," *IBM Journal of Research and Development*, vol. 37, no. 5, pp. 621-634, 1993.
- [27] Yuan J., and Falanga L., "The in-plane thermal expansion of glass fabric reinforced epoxy laminates", *Journal of Reinforced Plastics and Composites*, vol. 12, pp. 489-496, 1993.
- [28] IPC-TM-650 2.4.24.6, "Decomposition of laminate material using TGA", *The Institute for Interconnecting and Packaging Electronic Circuits*, Bannockburn, IL, April 2006.
- [29] IPC-TM-650 2.4.24.1, "Time-to-delamination (by TMA method)", *The Institute for Interconnecting and Packaging Electronic Circuits*, Northbrook, IL, December 1994.

- [30] IPC-TM-650 2.6.2.1A, "Water absorption, metal clad plastic laminates", *The Institute for Interconnecting and Packaging Electronic Circuits*, Northbrook, IL, May 1986.
- [31] Lambert, R., "The impact of materials on the flammability of printed wiring board products", *43rd Proceedings of Electronic Components and Technology Conference*, pp. 134 - 142, June 1993.
- [32] UL 94, "Tests for flammability of plastic materials for parts in devices and appliances", *Underwriters Laboratories*, June 1990.
- [33] Paterson-Jones J., Percy V., Giles R., and Stephen A., "The thermal degradation of model compounds of amine-cured epoxide resins. II. The thermal degradation of 1,3-diphenoxypropan-2-ol and 1,3-diphenoxypropene", *Journal of Applied Polymer Science*, vol. 17, no. 6, pp. 1877-1887, 1973.
- [34] Brito Z., and Sanchez G., "Influence of metallic fillers on the thermal and mechanical behavior in composites of epoxy matrix", *Composite Structures*, vol. 48, no. 1-3, pp. 79-81, 2000.
- [35] Sanchez G., Brito Z., Mujica V., and Perdomo G., "The thermal behavior of cured epoxy-resins: The influence of metallic fillers", *Polymer Degradation Stability*, vol. 40, no. 1, pp. 109-114, 1993.
- [36] Diamant Y., Marom G., and Broutman L., "The effect of network structure on moisture absorption of epoxy resins", *Journal of Applied Polymer Science*, vol. 26, pp. 3015-3025, 1981.
- [37] Levchik S., and Weil E., "Thermal decomposition, combustion and flame-retardancy of epoxy resins-a review of the recent literature", *Polymer International*, vol. 53, pp. 1901-1929, 2004.
- [38] <http://www.ptli.com/testlopedia/tests/FTIR-E168andE1252-more.asp> (accessed on 03/05/2008)
- [39] Luda M., Balabanovic A., and Camino G., "Thermal decomposition of fire retardant brominated epoxy resins", *Journal of Analytical and Applied Pyrolysis*, vol. 65, pp. 25-40, 2002.

- [40] Wang X., and Zhang Q., "Synthesis, Characterization, and cure properties of phosphorus-containing epoxy resins for flame retardance", *European Polymer Journal*, vol. 40, pp. 385-395, 2004.
- [41] Ren H., Su J., Wu B., and Zhou Q., "Synthesis and properties of a phosphorus-containing flame retardant epoxy resin based on bis-phenoxy (3-hydroxy) phenyl phosphine oxide", *Polymer Degradation and Stability*, vol. 92, pp. 956-961, 2007.
- [42] Ogi K., "Influence of thermal history on transverse cracking in a carbon fiber reinforced epoxy composite", *Advanced Composite Materials*, vol. 11, no. 3, pp. 265-275, 2003.
- [43] Wang Q., and Shi W., "Kinetics study of thermal decomposition of epoxy resins containing flame retardant components", *Polymer Degradation and Stability*, vol. 91, pp. 1747-1754, 2006.
- [44] Gundjian M., and Cole K., "Effect of copper on the curing and structure of dicy-containing epoxy composite system", *Journal of Applied Polymer Science*, vol. 75, pp. 1458-1473, 2000.
- [45] Liu Y., Hsiue G., Lan C., and Chiu Y., "Phosphorus-containing epoxy for flame retardance: IV. Kinetics and mechanism of thermal degradation", *Polymer Degradation and Stability*, vol. 56, pp. 291-299, 1997.
- [46] Marsh L., Lasky R., Seraphim D., and Springer G., "Moisture solubility and diffusion in epoxy and epoxy-glass composites", *IBM Journal of Research and Development*, vol. 28, no. 6, pp. 655-661, 1984.
- [47] Maggana C., and Pissis P., "Water sorption and diffusion studies in an epoxy resin system", *Journal of Polymer Science: Part B: Polymer Physics*, vol. 37, no. 11, pp. 1165-1182, 1999.
- [48] Ko M., and Kim M., "Effect of postmold curing on plastic IC package reliability", *Journal of Applied Polymer Science*, vol. 69, no. 11, pp. 2187-2193, 1998.

- [49] Gonon P., Sylvestre A., Teyseyre J., and Prior C., "Combined effects of humidity and thermal stress on the dielectric properties of epoxy-silica composites", *Materials Science and Engineering B*, vol. 83, no. 1-3, pp. 158-164, June 2001.
- [50] Aronhime M., Peng X., and Gillham J., "Effect of time-temperature path of cure on the water absorption of high  $T_g$  epoxy resins," *Journal of Applied Polymer Science*, vol. 32, pp. 3589-3626, 1986.
- [51] Wondraczek K., Adams J., and Fuhrmann J., "Effect of thermal degradation on glass transition temperature of PMMA", *Macromolecular Chemistry and Physics*, vol. 205, no. 14, pp. 1858-1862, 2004.
- [52] Sala G., "Composition degradation due to fluid absorption", *Composites Part B: Engineering*, vol. 31, no. 5, pp. 357-373, July 2000.
- [53] Smith C., "Water absorption in glass fiber-epoxide resin laminates", *Circuit World*, vol. 14, no. 3, pp. 22 -26, 1988.
- [54] Marsh L., Lasky R., Seraphim D., and Springer G., "Moisture solubility and diffusion in epoxy and epoxy-glass composites", *IBM Journal of Research and Development*, vol. 28, no. 6, pp. 655-661, 1984.
- [55] Flor G., Campari-Vigano G., and Feduzi R., "A thermal study on moisture absorption by epoxy composites", *Journal of Thermal Analysis and Calorimetry*, vol. 35, no. 7, pp. 2255-2264, November, 1989.